synthesis of modified Galacto- or Fuco-Clusters Exploiting the Siderophore Pathway to Inhibit the LecA- or LecB-Associated Virulence of Pseudomonas aeruginosa

Mimouna Madaoui, Olivier Vidal, Albert Meyer, Mathieu Noël, Jean-Marie Lacroix, Jean-Jacques Vasseur, Alberto Marra, François Morvan

Synthesis of modified galacto- or fuco-clusters exploiting siderophore pathway to inhibit LecA or LecB associated virulence of *Pseudomonas aeruginosa*

Mimouna Madaoui,[a] Olivier Vidal,[b] Albert Meyer,[a] Mathieu Noël,[a] Jean-Marie Lacroix,[b] Jean-Jacques Vasseur,[a] Alberto Marra[a] and François Morvan*[a]

[a]Institut des Biomolécules Max Mousseron (IBMM), CNRS, Université Montpellier, ENSCM, Montpellier, France, E-mail: francois.morvan@umontpellier.fr
[b]Unité de Glycobiologie Structurelle et Fonctionnelle (UGSF) - UMR 8576 CNRS - Université de Lille 1, Cité Scientifique, Avenue Mendeleiev, Bat C9, 59655 Villeneuve d'Ascq cedex, France

GRAPHICAL ABSTRACT

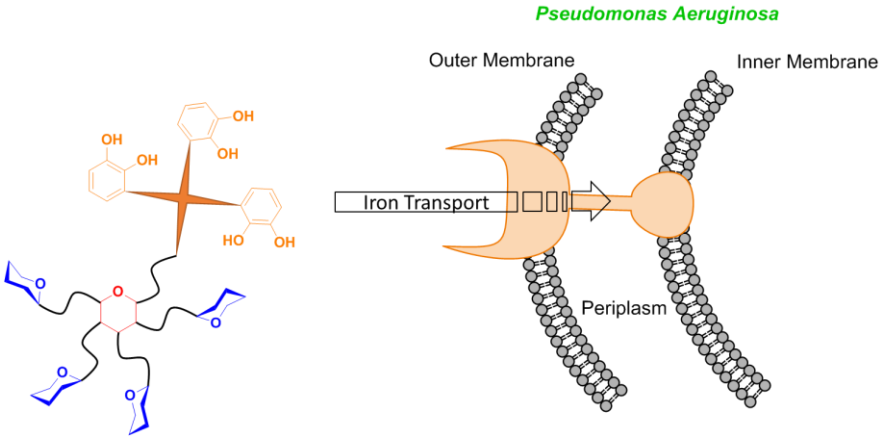

ABSTRACT

Galacto and fuco-clusters conjugated with one to three catechol or hydroxamate motifs were synthesized to target LecA and LecB lectins of *Pseudomonas aeruginosa* (PA) localized in the outer membrane and in the bacterium. The resulting glycocluster pseudosiderophore conjugates were evaluated as Trojan horse to cross the outer membrane of (PA) thanks to iron transport. The data suggests that glycoclusters with catechol moieties were able to hijack the iron transport while those with hydroxamates showed strong non-specific interactions. Mono- and tri-catechol galactoclusters (**G1C** and **G3C**) were evaluated as inhibitors of the infection by PA in comparison with the free galactocluster (**G0**). All of them exhibited an inhibitory effect between 46 to 75% at 100 mM with a higher potency than (?) **G0**. This result shows that LecA localized in the outer membrane of PA is involved in the infection mechanism.

INTRODUCTION

Bacterial infections with the appearance of antibiotics resistance lead to a severe problem of public health.[1] Alternative approaches to antibiotics are to be developed. To this end, glycoclusters exhibiting several epitopes recognized by the lectins of bacteria are supposed to perturb biofilm formation and bacteria cell recognition. They have been intensively synthesized.[2] These glycoclusters are designed to interact with high affinity with the lectins of bacteria thanks to the cluster effect.[3] *Pseudomonas aeruginosa* (PA), one of the most prevalent bacteria together with *S. aureus* and *E. coli*, is a Gram-negative, motile, opportunistic bacterium involved in nosocomial infections (10-30%).[4] This bacterium has two soluble lectins, LecA and LecB, that specifically recognize D-galactose and L-fucose, respectively, and are involved in its virulence and biofilm formation.[5] Furthermore, LecA has been shown to be involved in adhesion and intracellular uptake of the bacterium[6] and LecB is involved in adhesion on airway epithelial cells.[6a] Initially localized in the cytoplasm[7] both lectins were then largely found in the outer membrane of the bacteria.[5f]
To date, several glycoclusters, presenting of strong affinity for these two targets, have been reported in the literature[8] and some of them demonstrated some *in vivo* activity against PA especially antibiofilm property[8b, c, d , i, j, 9] and anti-bacterial adhesion.[8f, h, 10]

During the last few years, we have synthesized and evaluated in a DNA-based microarray, the affinity of hundreds of glycocluster-oligonucleotides bearing either D-galactose or L-fucose moieties and found some of them (Fig.1, Gal4 and Fuc4) with high affinity for those lectins.[11] The increase of affinity of galactoclusters determined by the measure of Kd by ITC[11b] was 400-fold higher than methyl β-D-galactoside, thanks to a cluster effect by chelation while the increase of potency of the fucocluster in comparison with monofucoside was lower (70-fold, IC_{50} determined by ELLA).[11a] Indeed, due to the shape of LecB, the increase of affinity is rather due to an increase of the local concentration of fucoside than to a chelation of two carbohydrate recognition domains (CRDs). The activity against biofilm formation has been established for two tetragalactoclusters leading to a 40% reduction of biofilm.[8b] In contrast, fucoclusters displaying high affinity for LecB were found unable to impair biofilm formation (unpublished results).

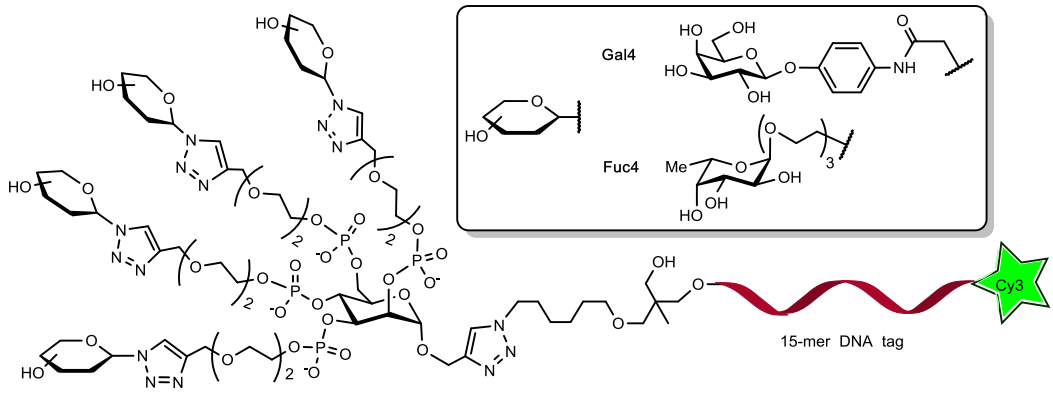

Figure 1 Structure of the **Gal4** and **Fuc4** glycocluster-oligonucleotides endowed with high affinity toward LecA and LecB lectins, respectively.

Iron is a key nutrient in bacteria and for all living systems, but due to the low solubility of iron(III) it is poorly available. To overcome this limitation, bacteria have developed siderophore-dependent iron acquisition systems.[12] Siderophores are low-molecular-weight iron chelators synthesized by bacteria mainly constituted of catechol or hydroxamate motifs.[12a, 13] The iron-siderophore complex is taken up by ferric-chelate specific TonB-dependent transporters allowing the transport of iron into bacteria.[14]

Several hundreds of microbial siderophores with different structures have been identified. The most potent siderophores are structurally based on catechol or hydroxamate moieties.[13]

Thus, it has been demonstrated that it is possible to hijack the transport of iron into bacteria for the uptake of antibiotics into bacteria leading to an increase of antibiotic potency (Trojan horse strategy).[15]

To our knowledge, this strategy has been only reported recently with the synthesis of calixarene-based glycoclusters against PA exhibiting four hydroxamate motifs.[9c] Most bacteria produce their own siderophores to catch iron from the medium, but they can also use xenosiderophores made by others microorganisms. Along this line PA, which synthesizes two major siderophores, pyoverdine (PVD) and pyochelin (PCH), is also able to use lot of xenosiderophores (siderophore piracy) like enterobactin, cepabactin, mycobactin and carboxymycobactin, desferrichrysin, desferricrocin, coprogen, vibriobactin, aerobactin, fungal siderophores and deferrioxamines (for a review see Cornelis, P., and Dingemans[16]).

RESULTS AND DISCUSSION

Since catechol and hydroxamate are the most represented motifs in siderophore, we decided to introduce them one to three times and evaluate their effect on the targeting of PA. The different

neosiderophores were conjugated to *galacto* and *fuco*-clusters and labelled with a fluorophore (Cy3) to visualize and quantify their interaction with the bacteria. As a control, the Cy3-glycocluster was also synthesized without a siderophore moiety. The resulting conjugates were evaluated on mutants to confirm or infirm the pathway through the siderophore active transport.

The syntheses of these bioconjugates were mainly performed on solid support using phosphoramidite chemistry and copper-catalyzed alkyne azide cycloaddition (CuAAC). Indeed, solid supported synthesis allowed a rapid synthesis of complex structures in low amount (< mg). This scale of synthesis produces enough material for a screening by fluorescence monitoring. Basically the glycocluster was synthesized and Cy3-labelled on solid support[17] then alkynes functions were introduced in the scaffold for a last conjugationperformed in solution with a catechol or a hydroxamate azide. Indeed, the catechol motifs were introduced in solution at the last step since they showed some instabilities under the ammonia treatment required to cleave the conjugate from the solid support. To this end, three new building blocks were synthesized: the di-acetyl catecholamide propylazide **3** (Scheme 1), the *O*-acetyl *N*-butylazide hydroxamate **7** (Scheme 2) and the *O*-DMTr-*O'*-levulinyl tris-hydroxylmethyl ethane (THME) cyanoethyl diisopropyl phosphoramidite **10** (Scheme 3).

Di-acetyl catechol propylazide **3** was synthesized in two steps starting from 2,3-dihydroxybenzoic acid on which 3-azido propylamine was coupled through an amide linkage using BOP/DIEA (50%). Then the hydroxyls were protected by treatment with acetic anhydride (54%) (Scheme 1). It is compulsory to protect the catechol hydroxyls since they are able to chelate the copper leading to an inefficient CuAAC and to some degradations.

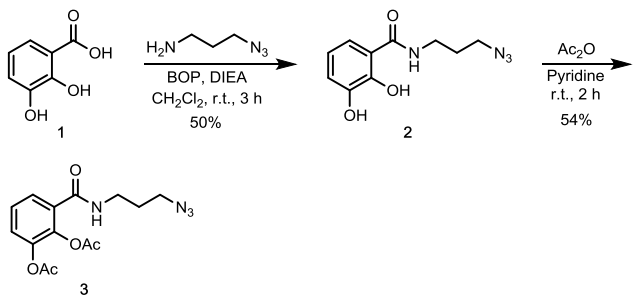

Scheme 1 Synthesis of *N*-(3-azidopropyl)-2,3-diacetoxy-benzamide (**3**).

Protected azidobutyl-hydroxamate **7** was obtained in three steps (Scheme 2). Acetohydroxamic acid **4** was first acetylated yielding **5**[18] which was secondly *N*-alkylated with 1,4-dibromobutane to give **6**. The third step was a substitution of bromine atom with azide by treatment with tetramethylguanidinium azide (TMG-N_3) affording **7**.

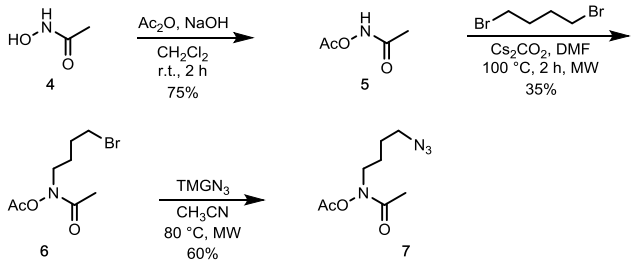

Scheme 2 Synthesis of *N*-(4-azidobutyl)-*N*-acetoxyacetamide (**7**).

In order to introduce a phosphoramidite derivative on a lateral chain of the scaffold, we synthesized the tris-hydroxylmethylethane (THME) phosphoramidite **10** protected on one hydroxyl with an acid labile dimethoxytrityl (DMTr) group and on a second hydroxyl with a hydrazine labile levulinyl (lev) group (Scheme 3). DMTr and Lev groups are orthogonal and so can be selectively removed allowing a selective reaction on a hydroxyl or on another with a subsequent phosphoramidite derivative. To this end, DMTr-THME **8**[19] was protected with levulinic acid by dicyclohexyl carbodiimide (DCC) activation and then the resulting compound **9** was phosphitylated by 2-cyanoethyl-*N*,*N*-diisopropylchloro phosphoramidite in presence of DIEA affording **10** (85%).

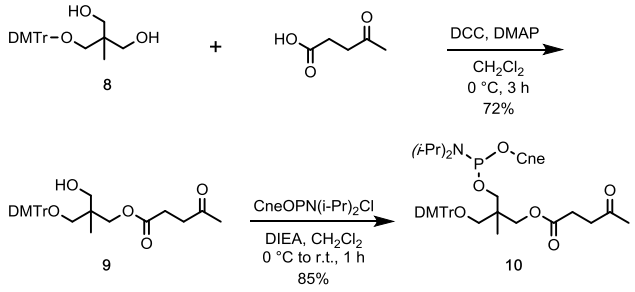

Scheme 3 Synthesis of the protected phosphoramidite **10**.

For the preparation of the control glycocluster without catechol/hydroxamate and the glycocluster with three catechol/hydroxamate the synthesis was identical for the first steps leading to **18** (Scheme 4). The propargyl α-D-mannoside **12**[20] was immobilized on azide solid support **11**[21] by CuAAc affording **13**[17] and the propargyl-diethyleneglycol phosphoramidite **14**[11a] was introduced on each hydroxyl to form **15** after oxidation of intermediate phosphite linkages. The DMTr group was removed by treatment with trichloroacetic acid (TCA) and the THME derivative protected with a levulinyl group **10** was introduced by solid phase phosphoramidite chemistry (SPPC) followed by a Cy3 phosphoramidite keeping its MMTr group. Levulinyl group was removed by treatment with a solution of hydrazinium acetate[22] leading to **16**. Then azide phenyl tetra-acetyl-galactoside **17a**[11a] was conjugated four times by CuAAC affording the solid-supported glycocluster **18**.

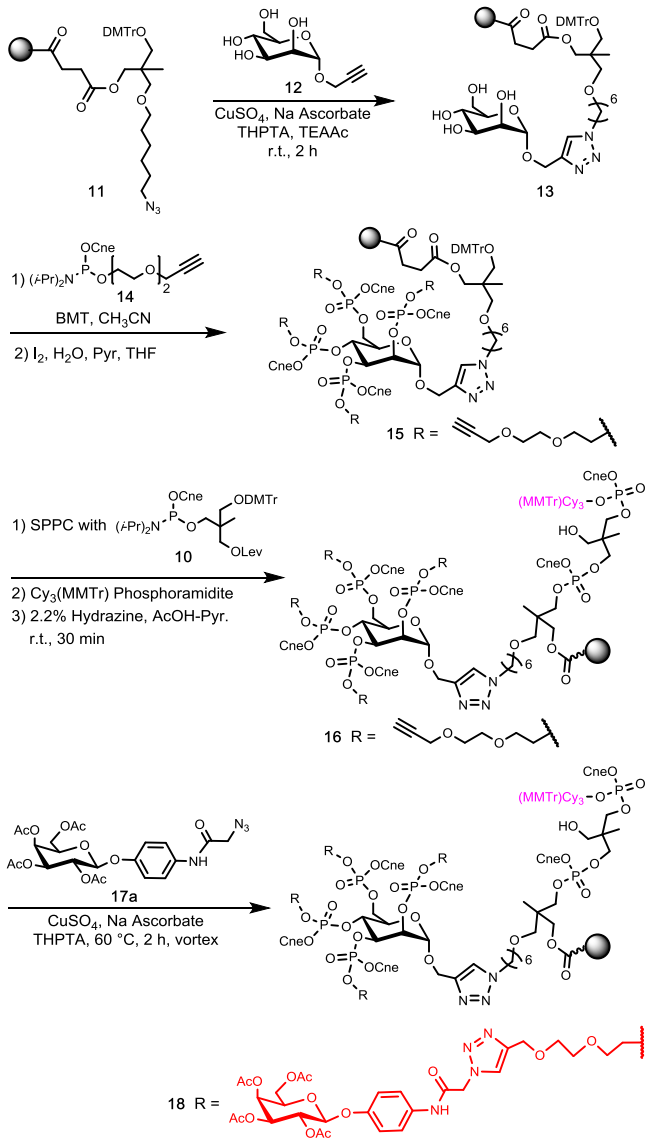

Scheme 4 Synthesis of solid-supported Cy3-glycocluster **18**. SPPC: i) 3% TCA in CH_2Cl_2; ii) amidite + benzylthiotetrazole (BMT), dry CH_3CN; iii) Capping: Ac_2O, *N*-methylimidazole, pyridine, THF; iv) 0.1M I_2, H_2O, THF, pyridine.

A portion of **18** was treated with TCA to remove the MMTr of Cy3 and finally with aqueous ammonia to give the control Cy3 labelled galactocluster (**^{cy3}G0**) (Scheme 5). The other portion of **18** was coupled with tris-propargyl pentaerythritol **19**[23] by solid phase phosphoramidite chemistry (SPPC) followed by deprotection with TCA and then aqueous ammoniagiving rise to Cy3-galactocluster **20** with three alkynes in solution. A last coupling with catechol azide **3** or hydroxamates azide **7**, followed by mild deacetylation afforded the galactocluster-tricatechol conjugate (**^{cy3}G3C**) or the galactocluster-trihydroxamate conjugate (**^{cy3}G3H**) respectively. The same strategy was applied for the synthesis of **^{Cy3}F0**, **^{Cy3}F3G** and **^{cy3}F3H** (Schemes S1-S2).

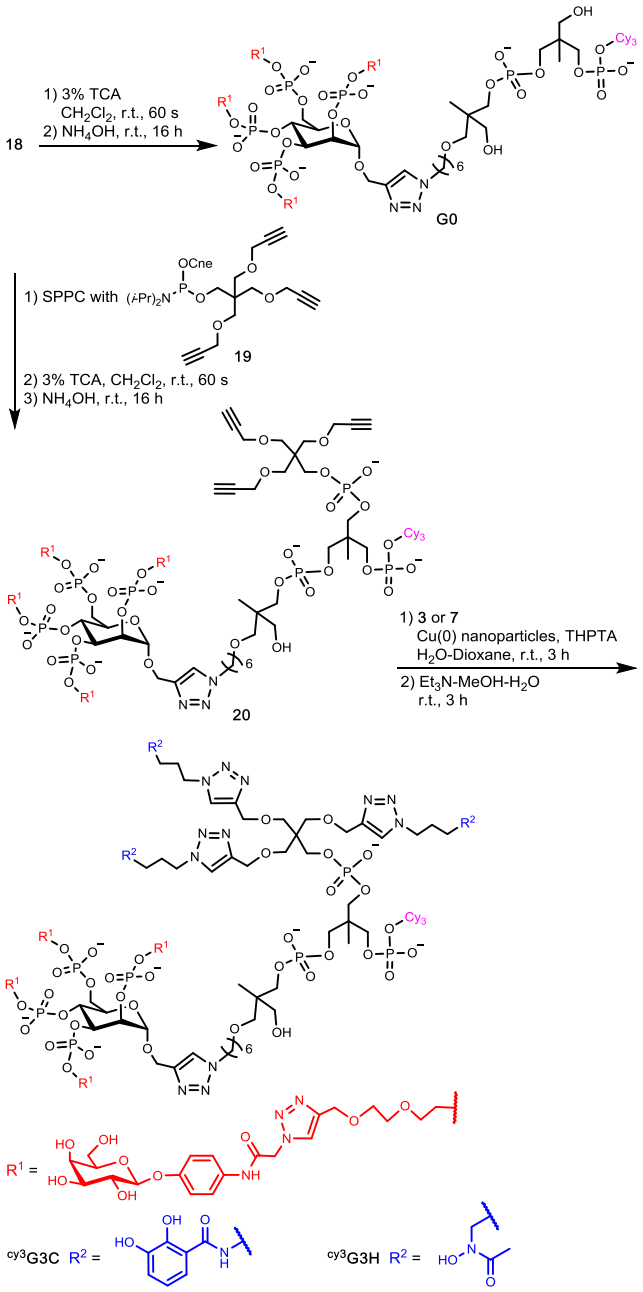

Scheme 5 Synthesis of Cy3-galactocluster without catechol (**^{cy3}G0**) and with three catechol (**^{cy3}G3C**) or three hydroxamates units (**^{cy3}G3H**).

For the synthesis of the mono- and di-catechol conjugates, the intermediate **15** was conjugated with fully protected galactoside azide **17a**, then the mono-propargyl **22a**[19] or the di-propargyl **22b**[24] phosphoramidite derivative were coupled by SPPC followed by Cy3 phosphoramidite coupling to give after ammonia deprotection **23a** and **23b** in solution respectively (Scheme 6). Finally, di-acetyl catechol propyl azide **4** or di-acetyl hydroxamate butyl azide **7** were conjugated by CuAAC affording after deacetylation the Cy3-galactoclusters mono- **^{cy3}G1C** and di-catechol **^{cy3}G2C**, and the corresponding Cy3-galactocluster mono- **^{cy3}G1H** and di-hydroxamate **^{cy3}G2H**.

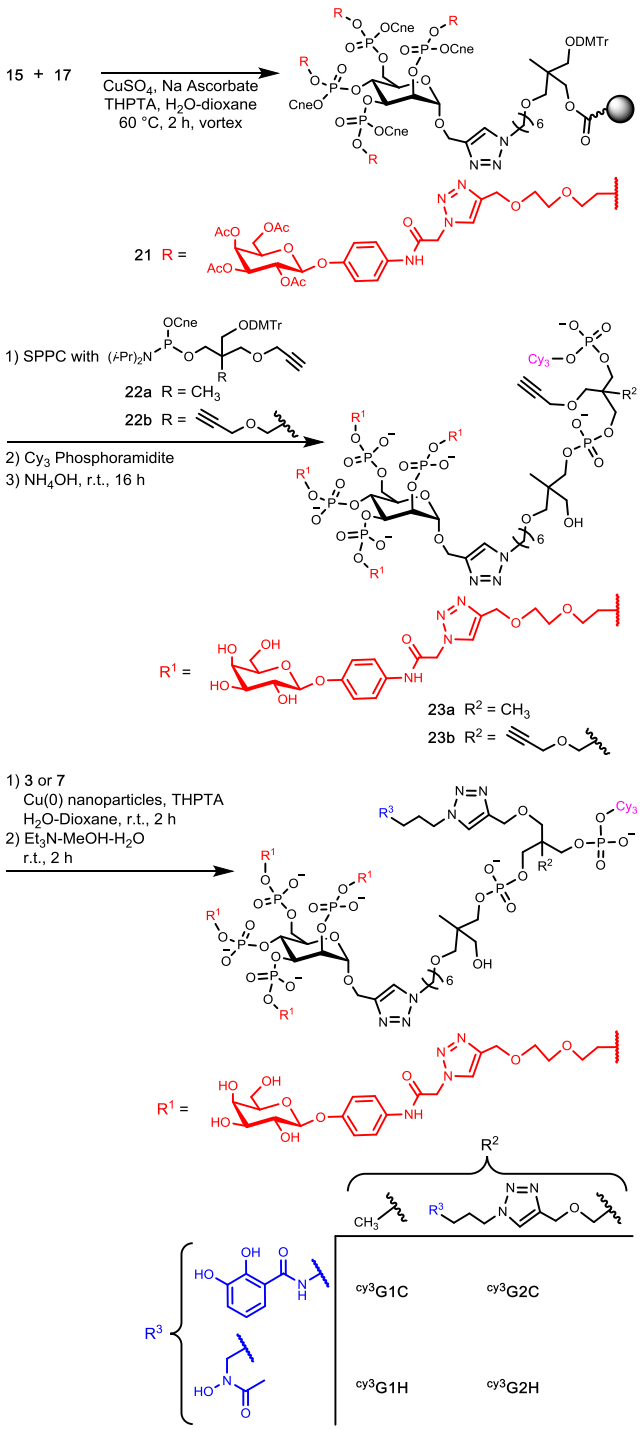

Scheme 6 Synthesis of the Cy3-galactoclusters with one (**^{cy3}G1C**) or two catechol (**^{cy3}G2C**) motifs and with one (**^{cy3}G1H**) or two (**^{cy3}G2H)** hydroxamate motifs.

For the synthesis of the fucoclusters, the same protocol was applied starting from **15** on which the fully protected fucoside azide **17b** was introduced yielding in fine the Cy3-fucoclusters mono- **^{cy3}F1C** and di-catechol **^{cy3}F2C** and the corresponding Cy3-fucocluster mono- **^{cy3}F1H** and di-hydroxamate **^{cy3}F2H** (Scheme S3).

The resulting 28 glycoclusters were characterized by C18 reverse phase HPLC and MALDI-TOF mass spectrometry. For the glycoclusters with catechols, HPLC profiles of acetylated derivative showed a thin peak while the fully deprotected compounds were eluted as a broad peak with and increasing complexity with the number of catechol motifs. This phenomenon could be explained by hydrogen bounding of the catechol with the stationary phase. In contrast the HPLC of glycoclusters with hydroxamates showed nice profiles. MALDI-TOF MS spectra showed only the $[M-H]^-$ ion corresponding to the expected structures.

Evaluation of labelling efficiency of *Pseudomonas aeruginosa* by galactocluster-siderophore conjugates.

The Cy3 fluorescence intensity of each glycocluster was measured. Indeed, it is known that catechol reduces the fluorescence intensity of fluorescent molecules.[25] While the fluorescence intensity of **^{cy3}G1C** was similar to that of **^{cy3}G0**, those of **^{cy3}G2C** and **^{cy3}G3C** were dramatically reduced by 78% and 96%, respectively (Fig. S4). One can imagine that such decrease of fluorescence is due to strong π,π interactions between the catechols and the indoles of Cy3 leading to non-radiative energy loss. For the fucoclusters series with catechols the decrease of fluorescent was lower with only 50% for **^{cy3}F3C** (Fig; S5). In contrast, the Cy3 fluorescence intensity of glycoclusters with hydroxamates motifs was increased by ~20% for **^{cy3}G1H** and **^{cy3}G2H** and by 15% for **^{cy3}G3H** with respect to **^{cy3}G0** (Fig. S6) while similar intensity was observed for **^{cy3}F0**, for **^{cy3}G1H** and **^{cy3}G2H** and slightly higher for **^{cy3}F3H** (Fig. S7). Explication de l'increase?

Fluorescence quantification of bacterial labelling by cy3-galacto/fucoclusters.

Trojan horse strategy is based on the use of the siderophore pathway to help entrance of inhibitors of virulence in the bacterial envelope to reach their specific target. We believed that such a strategy could help preventing LecA or LecB-dependant virulence of the bacteria by targeting the lectin before its exposure on the bacterial surface. Our first design of molecules was to simply add 1 to 3 catechol or hydroxamate residues on the galactocluster **G0** or fucocluster **F0** structure and to evaluate the potential of inhibition of the modified molecules. Synthesis of these molecules is expensive and time consuming. Consequently, only small amount of 1, 2 or 3 catechols-galacto/fucoclusters and 1, 2 or 3 hydroxamates-galacto/fucoclusters have been produced first and fluorescently labelled with cyanine (Cy3) to assess by fluorescence quantification their possible association with the bacteria.

The Cy3-galactocluster/fucocluster-siderophores were incubated with different PA strains: the wild type PAO1 and three isogenic mutants, *fpvA*, *exbB1* and *lecA* (galactoclusters) or *lecB* (fucoclusters). The Cy3-galactocluster-siderophores are expected to target LecA lectin (and

fucoclusters, LecB) associated with the bacterial cell surface as well as periplasmic/cytoplasmic LecA (LecB). *lecA* (*lecB*) mutant will then allow discrimination of non-LecA (LecB) specific labeling of the bacteria and should be considered as background. The *fpvA* mutant doesn't express the pyoverdine specific receptor (PVD-R) that recognizes pyoverdine and allows the active transport of iron-pyoverdine complex into the bacterium. Iron-pyoverdine recognition by FpvA is essentially due to association of the receptor with the chromophore(catecholate)/Fe/hydroxamates complex.[26] The Cy3-galacto(fuco)cluster-siderophores described herein don't share common structures with pyoverdine but have been designed to include 1 to 3 catechols or 1 to 3 hydroxamates residues. It has been described in the literature that antibiotics modified by the addition of catechols, cifedorocol[27] or hydroxamates, albomycins-like,[28] display better MIC (MIC défini?) than their non-modified counterpart demonstrating entrance of the antibacterial compounds *via* the siderophores uptake pathway. If in the experiments described here the *fpvA* mutant doesn't display any difference of Cy3-galacto(fuco)cluster-siderophores uptake than does the WT PAO1, no conclusions will be made. But if differences are observed they had to be attributed to entrance of the compounds via the FpvA receptor. The *exbB1* mutant is used herein for the same purpose. Siderophores-Fe entrance in the periplasm of the bacteria is dependent on energy transfer by the TonB/ExbB/ExbD cluster.[29] One can expect then that inactivation of the TonB/ExbB/ExbD machinery in *Pseudomonas aeruginosa* will lead as well as a reduction of galacto(fuco)cluster-siderophores entrance in the bacterial envelope.

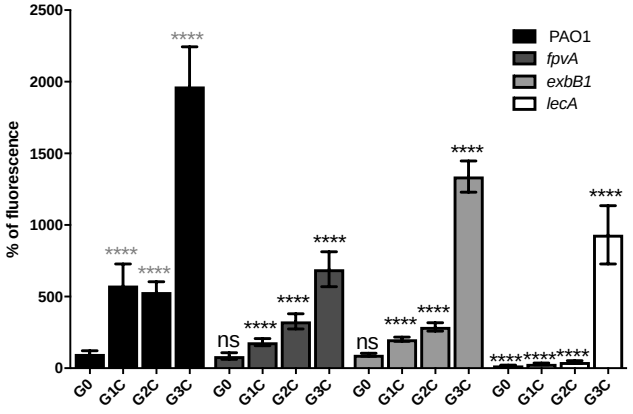

Figure 2. Percentage of labelling of PA strains with 1 µM Cy3-galactocluster with 0 to 3 catechols. Data were normalized to 100% for the Cy3-galactocluster with 0 catechols (**G0**) added to the wild type strain PAO1. Grey "*" are statistical comparison between **G0** and 1, 2, or 3 catechols for the PAO1. Black "*" are statistical comparison of each mutant, *lecA*, *exbB1* or *fpvA* labelled with Cy3-galactocluster with 0, 1, 2 or 3 catechols respectively to the corresponding PAO1 labelled with Cy3-galactocluster with the same number of catechols (0 to 3 catechols). With *, $p<0.05$; **, $p<0.01$; ***, $p<0.001$; ****, $p<0.0001$.

The data were normalized with a percentage of labelling fixed at 100% for **^{cy3}G0** (1 **µ**M) when incubated with wild type PAO1 (Figure 2). The **^{cy3}G1C** and **^{cy3}G2C** exhibited a 5-fold increase of labelling and the **^{cy3}G3C** showed a strong increase of 20-fold. Thus, the addition of 1 to 3 catechol residues on the galactoclusters structure increase its association with the WT bacterial envelope.
When the galactoclusters were incubated with *lecA* mutant we observed a very low labelling for **^{cy3}G0**, **^{cy3}G1C** and **^{cy3}G2C** showing no interaction of the galactocluster with the mutant devoid of LecA synthesis. Initial works of Glick and Garber have located the soluble LecA lectin mainly in the cytoplasm of the bacteria with a small percentage (3-9%) membrane bound or located in the periplasmic space.[7] Membrane localisation of LecA was confirmed by one other group.[30] However, how did the lectin come in the envelope of the bacteria still remains unknown since the lecA gene doesn't contain any specific signal peptide encoding sequence.[30] Difference of labelling observed here between PAO1 and the *lecA* mutant must signify specific association of galactoclusters with or without catechols with the target LecA and its location in the bacterial envelope.

When the mutants *fpva* and *exbB1* were incubated with Cy3-galactocluster catechol conjugates and **^{cy3}G0**, we observed the same level of labelling for **^{cy3}G0** and a strong decrease of labelling for the **^{cy3}G1C**, **^{cy3}G2C** and **^{cy3}G3C** showing that the high labelling on PAO1 was due to some interaction between Cy3-galactocluster catechol conjugates and the iron transport mechanism. Increase of fluorescence labelling of the bacteria with catechols-Cy3-galactoclusters compared to Cy3-galactoclusters is not alone a direct proof of the entrance of the molecules in the bacterial envelope via the siderophore pathway. One may argue that it could be the result of unspecific interaction of the catechols with the bacterial envelope. As example, **^{cy3}G3C** also displayed a high labelling of the *lecA*, *fpvA* and *exbB1* mutants even if it is 1,5 to 3-fold less than for wild-type PAO1. This phenomenon would be due to some non-specific adsorption of **^{cy3}G3C** on the surface of bacteria rather than some internalization of it thanks to iron transport due to the recognition of the three-catechol motif by the bacteria. But, since *lecA*, *fpvA* and *exbB1* mutants are isogenics of PAO1 strain, the decrease of labelling observed is obviously due to the absence of membrane associated LecA for the *lecA* mutant and absence of a functioning siderophore pathway for the two latter. Consequently, as expected, our data show that addition of 1 to 3 catechol residues allows entrance of the Cy3-galactocluster in the bacterial envelope via the siderophore pathway. Then, higher amount of the molecules has been produced to assess its inhibitory potential against PA virulence.

In contrast to the Cy3-galactoclusters-catechol conjugates ^{Cy3}**G1C** and ^{Cy3}**G2C**, the Cy3-fucoclusters-catechol conjugates ^{Cy3}**F1C** and ^{Cy3}**F2C** showed a low increase of fluorescence for the control strain while ^{cy3}**F3C** showed a large increase (16-fold) (Figure S8). Surprisingly, the percentage of labelling observed for ^{Cy3}**F0** are similar for the WT and for the mutant *lecB* suggesting no specific interaction with the membrane bound lectin. In vitro experiments, has shown that **F0** is highly affine for LecB[34] but no interaction with membrane bound LecB has been demonstrated to date. Tielker and coworkers[11] have demonstrated localization of LecB in the PA outer membrane where its presence helps biofilm development. Thus, our result indicates that the fucoclusters developed herein don't interact with membrane bound LecB in vivo.

For the WT strain and the *fpvA* mutant we observed a higher labelling for ^{cy3}**F3C** when the others mutants, *exbB1* and *lecB,* were low and similar. Difference between labelling of the *fpvA* and *exbB1* mutant suggest interaction of ^{cy3}**F3C** with the siderophore pathway independent of the pyoverdin uptake. Additionally, difference of ^{cy3}**F3C** labelling between WT and the *lecB* mutant suggests that interaction with the siderophore pathway helps the fucocluster to reach soluble LecB to interact with confirming that three catechol residues enhance association of the glycocluster with siderophore pathway. Nevertheless, since the control molecule ^{cy3}**F0** doesn't show any difference of labelling between WT and *lecB* mutant no further experiments were conducted with fucoclusters-catechol conjugates.

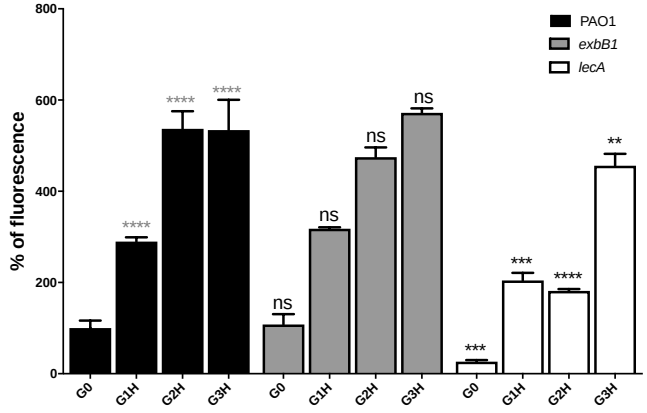

Figure 3. Percentage of labelling of PA strains with 1 μM Cy3-galactocluster with 0 to 3 hydroxamate. Data were normalized to 100% for the Cy3-galactocluster with 0 hydroxamate (**G0**) added to the wild type strain PAO1. Grey "*" are statistical comparison between **G0** and 1, 2, or 3 hydroxamate for the PAO1. Black "*" are statistical comparison of each mutant, *lecA* or *exbB1* labelled with Cy3-galactocluster with 0, 1, 2 or 3 hydroxamate respectively to the corresponding PAO1 labelled with Cy3-galactocluster with the same number of hydroxamate (0 to 3 hydroxamate). With *, $p<0.05$; **, $p<0.01$; ***, $p<0.001$; ****.

The Cy3-galactocluster hydroxamate conjugates **^{cy3}G1H**, **^{cy3}G2H** and **^{cy3}G3H** as well as **^{cy3}G0** were incubated with PAO1, *exbB1* and *lecA* (Figure 3). The labelling of PAO1 increased by 3-fold for **^{cy3}G1H** and by almost 6-fold for **^{cy3}G2H** and **^{cy3}G3H** with respect to **^{cy3}G0**. As for the catechol series, the highest substituted hydroxamate glycoconjugate exhibited the highest labelling. However, surprisingly, for the *exbB1* mutant the increase of labelling was similar showing that the increase of labelling should not be due to some interaction of the galactoclusters with the iron-transport mechanism. ExbB1 is not interacting with is hydroxamate glycoconjugate, since it is a more general partner of the siderophore uptake than FpvA (restricted to the pyoverdin-like molecules uptake) the *fpvA* mutant has not been tested. Finally, the labelling of the lecA mutant was also found to be increased but to a lower extent.

The same trend was observed for the fucocluster-hydroxamate conjugates with a high non-specific interaction when the number of hydroxamate motifs increased (Figure S9) but also an absence of interaction with the siderophore pathway.

All the data suggested that there are some non-specific interactions of the Cy3-galactocluster or fucocluster hydroxamate conjugates with the bacteria and that the hydroxamate motifs reported in this study are not recognized by the bacteria as a siderophore.

To summarize this first study, the data show that catechol-galactoclusters were internalized by iron-assisted transport while hydroxamate glycoclusters were not. For the fucocluster-catechol conjugates, the increase of labelling was not really significant and it seems that the fucocluster was not recognized by LecB while fucocluster-hydroxamate conjugates showed high non-specific interaction. Hence, for the evaluation of the anti-infectious properties of glycoclusters on bacteria, we only selected the monocatechol galactocluster, since there is a similar behaviour between **G1C** and **G2C**, and the tri-catechol galactocluster **G3C** to evaluate the effect of the number of catechol on the activity.

Solution phase synthesis of mono- and tri-catechol glycoclusters G1C and G3C

The syntheses were performed in solution to obtain few hundred milligrams of each compound. Since we observed some instability of acetyl groups on catechol, the more stable benzoyl group was selected. 2,3-Dihydroxybenzoic acid was first protected by treatment with benzoic anhydride to give **24**. The carboxylic function was activated as an anhydride by treatment with ethyl chloroformate and eventually 3-azido-propylamine was added to form the amide linkage affording the *N*-(3-azidopropyl)-2,3-dibenzoxybenzamide **25** in 62% overall yield (Scheme 7).

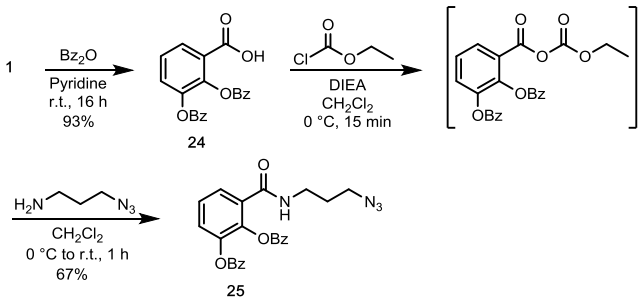

Scheme 7 Synthesis of *N*-(3-azidopropyl)-2,3-dibenzoxy-benzamide **3**.

The monocatechol-glycocluster **G1C** was synthesized in four steps (Scheme 8). Protected catechol derivative **25** was conjugated by CuAAc to propargyldiethyleneglycol α-mannoside **26**[31] and the free hydroxyls were phosphorylated by means of propargyldiethyleneglycol phosphoramidite **14** followed by oxidation with solid-supported A26 IO_4^- reagent to give **28**. The galactoside units were finally introduced by CuAAC to afford **G1C** after deprotection.

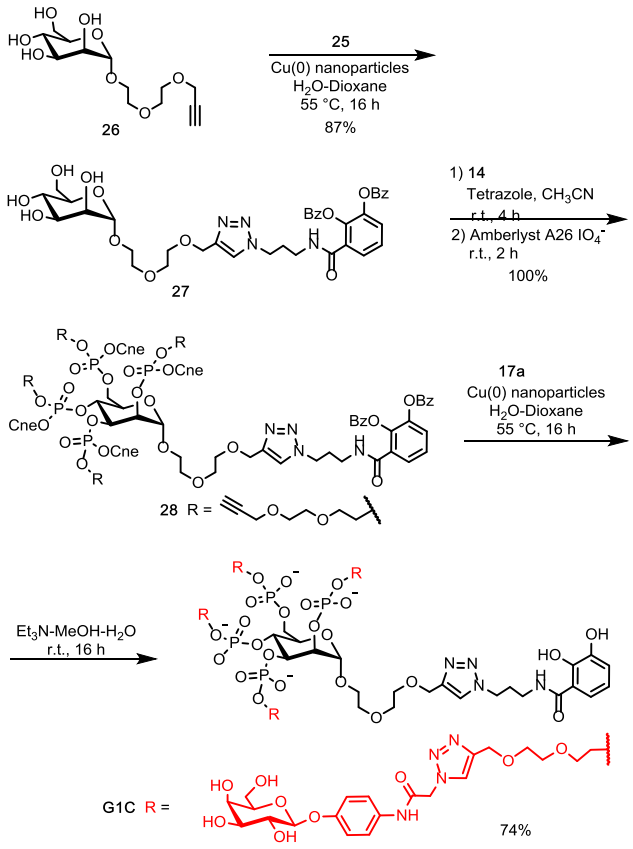

Scheme 8 Synthesis of glycoclusters **G1C** in solution.

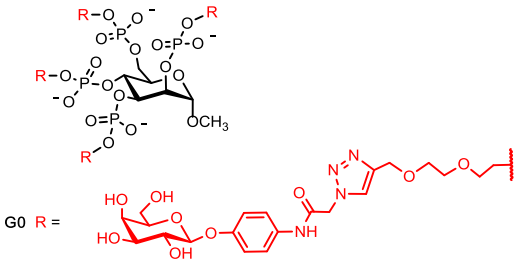

Figure 4 Structure of glycocluster **G0**.

The synthesis of **G3C** was carried out according to a convergent strategy. The galactocluster **32** was synthesized with a propargyl diethyleneglycol arm on the anomeric carbon of mannoside (Scheme 9) and the tricatechol **37** was synthesized with an azide diethyleneglycol arm (Scheme 10) allowing a final conjugation of both units **32** and **37** (Scheme 11).

Since the mannoside **26** exhibited an alkyne function, it was not possible to first introduce propargyl diethyleneglycol phosphoramidite on it and then the azide galactosides. Hence the azide tetraacetylgalactoside **17a** was conjugated by CuAAC to propargyl diethyleneglycol and then converted to its phosphoramidite derivative **30** which was coupled with **26** affording the alkynyl-galactogluster **31** which was finally deprotected to give **32**.

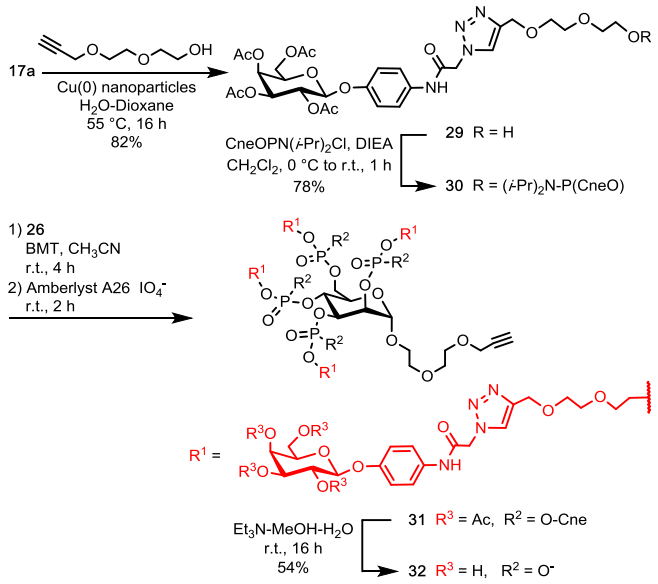

Scheme 9 Synthesis of the alkynyl-galactocluster **EG_2**.

For the siderophore synthesis, the tripropargyl-pentaerythritol **33** was coupled to tosyltriethyleneglycol phosphoramidite **34** and after oxidation of phosphite triesters into phosphotriesters the three catechols were introduced by CuAAC affording **35** (Scheme 10). Since

during azidation debenzoylation was observed, **35** was first deprotected and azidation was performed by treatment with TMG azide. Finally the hydroxyls were reprotected by treatment with benzoyl chloride affording the azide-sidererophore **37**. The perbenzoylation using benzoyl anhydride was inefficient and led with benzoyl chloride to a partial side reaction . Indeed, we have observed to a certain extent the formation of a secondary product corresponding to the loss of a catechol carboxy acid and a benzoylation of the intermediate amine. This side reaction is surprising since amides of aliphatic amines are usually very stable.

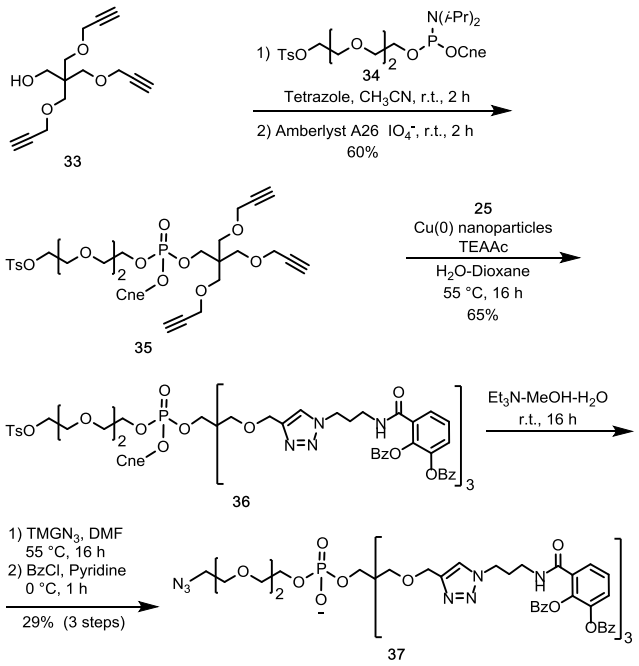

Scheme 10 Synthesis of the azidated tricatechol derivative **37**.

A last CuAAC conjugation allowed the formation of benzoylated **G3C** (Scheme 11). Surprisingly the reaction was very sluggish requiring 6 days. A reduced accessibility of the azide and alkyne functions with the two quite large units could explain the slowness of the click reaction . After chromatography on C18 reverse phase and deprotection **G3C** was afforded.

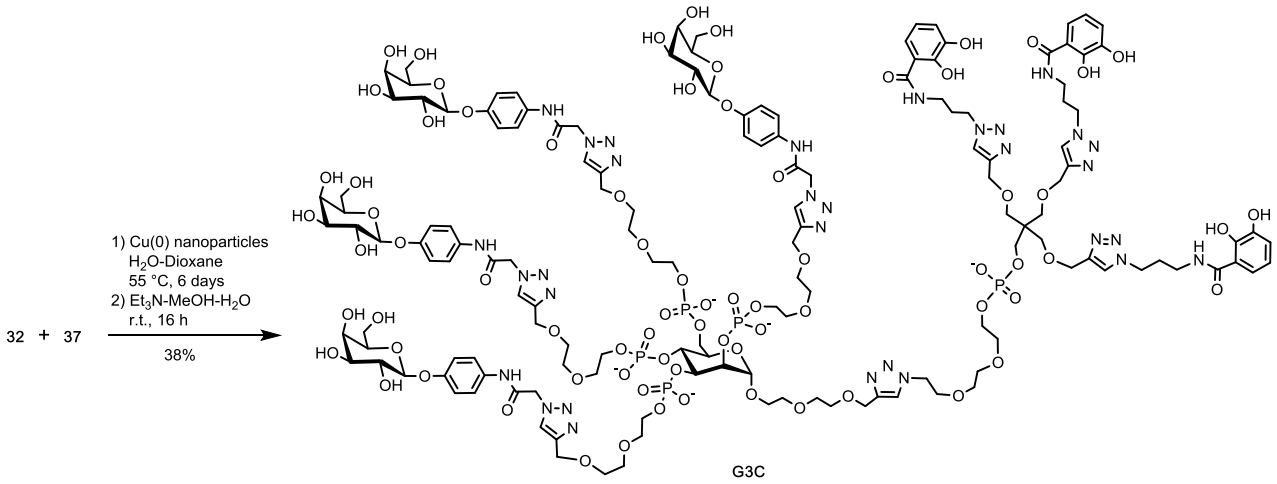

Scheme 11 Synthesis of the galactocluter-tricatechol **G3C**.

Infection protection assay with G0, G1C and G3C

The monocatechol **G1C** and tricatechol **G3C** galactoclusters were tested as inhibitors of infection in comparison with the glycocluster **G0** (Figure 4).[8b] Various concentrations of each inhibitor were tested in order to demonstrate dose dependant inhibition of infection (Figure 5).

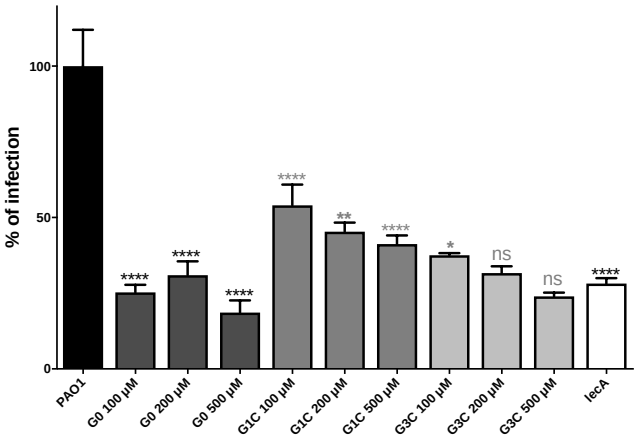

Figure 5. Inhibition of PAO1 infection using **G0**, **G1C**, and **G3C** at concentration ranging from 100 to 500 µM compared to the *lecA* mutant. Data were normalized to 100% for the WT strain PAO1. Black "*" are statistical comparison between PAO1 and G0, and *lecA* wile grey "*" were statistical comparison between G0 and G1C and G3C. With *, p<0,05 ; **, p<0,01 ; ***, p<0,001 ; ****, p<0,0001.

As expected, compared to PAO1, *lecA* mutant displays a lower infection percentage with only 28±14 % of the WT infection percentage. Concentrations of galactocluster **G0** ranging from 100 to 500 µM reduce up to 70% the percentage of infection of PAO1. Thus 100 µM of **G0** is already sufficient to reduce the whole LecA dependant percentage of infection for the PAO1 strain. Increase

of the **G0** concentration in the medium doesn't increase the level of inhibition since probably all the LecA exposed on the surface of the bacterial cell is already masked by 100 μM of the galactocluster. Lower concentration of the galactoclutser **G0** decreases the efficiency of inhibition since 10 μM only reduce to 25% (76±21 %) the percentage of infection of PAO1 (data not shown).

In a previous work, we have demonstrated that galactoclusters (**G0**), targeting the soluble LecA lectin of *Pseudomonas aeruginosa* (PA), when added in a concentration as low as 10 μM, can reduce considerably (up to 40%) the biofilm development of the bacteria.[8b] Several similar molecules were developed by other groups showing equivalent results[8b-d, 8i, j, 9] demonstrating the importance of the lectin during the biofilm building even if it is still not very clear how the lectin can help its development. LecA involvement in PA virulence is a lot more complex since the lectin was shown to display on his own cytotoxic effect on respiratory epithelial cells[32] and acts, associated to the bacteria, as an adhesin[5f]/invasin[6a] to host tissue by directly binding to the globotriosyl receptor (Gb3)[6a] promoting cell infection by the bacteria.

In the present work, we show that 100 μM of galactoclusters (**G0**) is sufficient to reduce up to 70% the PA infection in an ex-vivo model of infection using the human pulmonary cell line NCI-H292. Increased concentration of the inhibitor doesn't increase the inhibition efficiency suggesting that the maximum inhibitory potential was reached. Infection done with the *lecA* mutant strain has also shown a 70% reduction compared to the WT which mean that 30% of the PA infection potential is independent of LecA.
Our previous publication has shown that 130 μM of the galactocluster **G0** decreases the adhesion force existing between PA and fixed cells on an AFM tip.[10b] The combined results suggest that galactoclusters prevent host cell Gb3 LecA dependent recognition by the bacteria diminishing the infection ratio.
Such a 70% inhibition of PA ability to colonize pulmonary cell ex-vivo using β-D-galactopyranoside-presenting glycoclusters was also observed by Malinovská and co-workers using higher concentrations of inhibitor (up to 2 mM).[10c] The galactoclusters developed herein seem, up to date, being more efficient to reduce PA infection on pulmonary cells and should be good candidates to further in vivo protection assay in an animal model.

Unfortunately, addition of one or three catechols on the galactocluster structure (**G1C** and **G3C**) doesn't increase the inhibition potential of the molecule as compared to **G0** with even a percentage of infection observed for 100 μM of **G1C** (54±20 %) or **G3C** (38±5 %) higher than that observed for **G0** (25±5 %).

Since no direct proof of entrance of the molecules in the cytoplasm of the bacteria was demonstrated in our work, we can't rule out the fact that simply the inhibitor doesn't reach intracellular LecA to increase the inhibition efficiency. One may argue that the presence of catechols could decrease affinity of the galactocluster for membrane bound LecA or the stability of LecA/galactocluster complex. It is possible that the ability of catechols to interact with divalent cations may have competed with the affinity of LecA with Ca^{2+} necessary for the LecA/galactose interaction.

Our experiments show that the addition of one or three catechols promotes entrance of the galactoclusters in the bacterial envelope via the siderophore pathway. Thus, one other interpretation will be that the catechol-galactoclusters reach its intracellular LecA target but that this has no influence on the bacterial virulence since during the two hours of infection only the membrane bound LecA is used by the bacteria during the infection process.

According to Diggle and coworkers, membrane bounds LecA may have come from other bacterial cell lysis, liberating soluble lectin which then link to the bacterial surface and help virulence.[30] Then, LecA binding on Gb3 receptor exposed on host cell surface will allow engulfment of the bacteria and cell infection.[13] This model can explain why only a few percentage of LecA is membrane bound, how it came here, and why bacterial free LecA displays cytotoxic effect on host tissue. In addition, this may also explain why, as this work shows, the force entry of the galactocluster targeting LecA into the bacterial envelope by Trojan horse strategy, did not succeed in improving its inhibition potential.

CONCLUSION

The purpose of the present work was to develop inhibitors of PA virulence by targeting the lectins LecA and LecB involved in biofilm formation and host tissue infection. Since the two lectins are mostly cytoplasmic and only around 5% membrane bound, Trojan horse strategy based on catechol- or hydroxamate-modified galacto/fucoclusters mimicking siderophores has been developed to help the inhibitors to reach the largest possible amount of lectin targets. Our results show that only galactocluster-catechol conjugates were able to penetrate the bacterial envelope via the siderophore pathway. Protection assays of human pulmonary cell culture against PA infection using galactoscluster **G0** or its catechols (**G1C** and **G3C**) associated counterparts have been successful in this work comforting us in the efficiency of galactoclusters as inhibitor of PA virulence. As discussed above, although the protection assays with **G0** at micromolar concentration led to very interesting results, the assays with catechol-galactoclusters were disappointing, because no gain compared to **G0** and even a reduction of the inhibitor efficiency was observed. Nevertheless,

evidences have been gained that addition of 1 to 3 catechols promotes entrance of chemical compounds into PA envelope via the siderophore pathway and can be suitable for other inhibitors.
Finally, this work shows that the Trojan horse strategy targeting LecA is not helpful against PA virulence. On other hand, we proved that 100 μM of **G0** added in the culture medium were sufficient to reduce PA virulence to a same extent as the *lecA* mutant. If the virulence of the bacteria is in fact promoted by non-membrane bound LecA, soluble galactoclusters, such as **G0**, recruiting soluble, bacterial free, LecA in the tissue neighbourhood and preventing their further association either with bacterial or cell membrane can certainly help to protect against PA infection.

EXPERIMENTAL SECTION

All reagents for synthesis were commercial and used without purification. Dry solvents and reagents CH_3CN, pyridine, DIEA and NEt_3 were distilled over CaH_2 and CH_2Cl_2 was distilled over P_2O_5, others solvents were commercial and used without distillation. Sensitive reactions were performed under argon atmosphere. Reactions under microwaves were achieved on Monowave 300 Anton Paar. The reactions were monitored by TLC using silica gel 60 F_{254} precoated plates. TLC plates were analysed by UV light (λ = 254 nm) and revealed by treatment with $KMnO_4$, Ninhydrine in EtOH, 10% H_2SO_4 in EtOH/H_2O (1:1 v/v), phosphomolybdic acid 20 wt% solution in EtOH or molibdenum blue according to Dittmer and Lester followed by heating. Products were purified on silica gel column chromatography with silica gel Si 60 (40-63 μm) or silica gel flash chromatography (35-45 μm). Reverse phase purification was executed with C_{18} flash chromatography (40 μm). Reverse phase C_{18} HPLC analyses were performed with Dionex Ultimate 3000 instrument equipped with an automatic injector and a photometer DAD 3000 with Nucleodur® 100 Å, 3 μm C18ec, 75 mm DI 4.6 mm, Macherey-Nagel column (flow 1 mL/min using linear gradient of CH_3CN in 0.05M aqueous TEAAc pH 7). NMR analyses were performed at 298 K using a 200 MHz, 400 MHz, 500 MHz or 600 MHz spectrometer (Bruker) using deuterated solvent. Observed multiplicities are labelled with following abbreviation: s (singlet), d (doublet), dd (doublet of doublet), t (triplet), tt (triplet of triplet), q (quartet), p (quintet), m (multiplet). Shifts (δ) were referenced relative to deuterated solvent and expressed in part per million (ppm), coupling constants were expressed in hertz (Hz). High resolution (HR-ESI-QTOF) mass spectra were achieved with Q-Tof Micromass spectrometer. MALDI-TOF analysis were performed on a Shimadzu Assurance equipped with 337 nm nitrogen laser. Spectra were recorded, in negative or positive mode, using THAP with 10% of ammonium citrate as a matrix in water CH_3CN (1:1 v/v). Liquid samples were mixed with the matrix as 1:5 v/v ratio and 1 μL was deposited on the stainless-steel plate for drying.

***N*-(3-azidopropyl)-2,3-dihydroxybenzamide 2:** 2,3-Dihydroxybenzoic acid (894 mg, 5.8 mmol) was dissolved in anhydrous CH_2Cl_2 (17 mL), 3-azidopropylamine (701 mg, 7 mmol) and anhydrous DIEA (2 mL, 11.6 mmol) were added and the mixture was dried over molecular sieve 4Å for 1h under argon and cooled down to 0 °C. BOP (2.6 g, 5.8 mmol) was added and the solution was stirred for 3h at room temperature. The crude was directly applied on a silica gel column for flash chromatography using cyclohexane with AcOEt (from 20% to 80%). Product was lyophilized from dioxane to afford compound **2** (716 mg, 50%) as a colorless oil. TLC Rf: 0.53 Cyclohexane: AcOEt 4:6 v/v. ^{1}H NMR (400 MHz, $CDCl_3$) δ 12.65 (s, 1H, OH), 7.05 (dd, *J* = 7.8, 1.2 Hz, 1H, Ar), 6.89 (dd, *J* = 8.1, 1.1 Hz, 1H, Ar), 6.76 (t, *J* = 8.0 Hz, 1H, Ar), 6.66 (s, 1H, NH), 5.86 (s, 1H, OH), 3.56 (q, *J* = 6.4 Hz, 2H, N$\underline{CH_2}CH_2$), 3.47 (t, *J* = 6.4 Hz, 2H, $CH_2\underline{CH_2}N_3$), 1.91 (p, *J* = 6.4 Hz, 2H, $\underline{CH_2}CH_2N_3$). ^{13}C NMR (101 MHz, $CDCl_3$) δ 170.3, 149.2, 146.1, 118.9, 118.3, 116.0, 114.3, 49.8, 37.7, 28.6. HR-ESI-QToF MS (positive mode): m/z calcd. for $C_{10}H_{13}N_4O_3$ $[M+H]^+$ 237.0988, found 237.0991.

***N*-(3-azidopropyl)-2,3-diacetoxybenzamide 3:** *N*-(3-azidopropyl)-2,3-dihydroxybenzamide **2** (385 mg, 1.63 mmol) was solubilized in anhydrous pyridine (10 mL) and acetic anhydride (3.0 mL, 32.6 mmol) was added. The solution was stirred for 2h at room temperature. AcOEt was added (100 mL) and organic layer was washed twice with a 1M HCl aqueous solution (2 x 60 mL), twice with a saturated solution of $NaHCO_3$ (2 x 60 mL) and once with brine (60 mL). Organic layer was dried over Na_2SO_4 and solvent was evaporated under vacuum. The crude was purified by silica gel flash chromatography using cyclohexane and AcOEt (from 20% to 50%) to afford compound **3** (284 mg, 54%) as a white solid. TLC Rf: 0.22 Cyclohexane/EtOAc (4:6 v/v). ^{1}H NMR (400 MHz, $CDCl_3$) δ 7.53 (dd, *J* = 6.1, 3.3 Hz, 1H, Ar), 7.30 – 7.27 (m, 2H, Ar), 6.39 (t, J = 6.6 Hz, 1H, NH), 3.46 (q, *J* = 6.6 Hz, 2H, N$\underline{CH_2}CH_2$), 3.40 (t, *J* = 6.6 Hz, 2H, $CH_2\underline{CH_2}N_3$), 2.31 (s, 3H, OC$\underline{CH_3}$), 2.29 (s, 3H, OC$\underline{CH_3}$), 1.84 (p, *J* = 6.6 Hz, 2H, $NCH_2\underline{CH_2}CH_2N_3$). ^{13}C NMR (101 MHz, $CDCl_3$) δ 168.2, 168.1, 165.4, 143.1, 140.2, 130.5, 126.7, 126.5, 125.9, 49.4, 37.7, 28.8, 20.7, 20.6. HR-ESI-QToF MS (positive mode): m/z calcd. for $C_{14}H_{17}N_4O_5$ $[M+H]^+$ 321.1199, found 321.1200.

***N*-acetoxyacetamide 5**:[18] Acetohydroxamic acid **4** (1.0 g, 13.3 mmol) was dispersed in heterogeneous mixture of CH_2Cl_2/NaOH 2M (1:1 v/v 14 mL). Acetic anhydride (1.9 mL, 19.9 mmol) was added and the mixture was stirred at room temperature for 2h. Aqueous layer was extracted four times with CH_2Cl_2. Organic layer was dried over Na_2SO_4 and solvent evaporated (yellow oil). Product **5** was obtained as a colorless oil (1.17 g, 75%) after purification by chromatography on silica gel using CH_2Cl_2 with 0 to 5% of MeOH. TLC Rf: 0.35 CH_2Cl_2/MeOH (95:5 v/v). ^{1}H NMR (400 MHz, $CDCl_3$) δ 9.13 (s, 1H, NH), 2.22 (s, 3H, CH_3), 2.05 (s, 3H, CH_3).

^{13}C NMR (101 MHz, $CDCl_3$) δ 169.0, 19.8, 18.4. HR-ESI-QToF MS (negative mode): m/z calcd for $C_4H_6NO_3$ $[M-H]^-$ 116.0348, found 116.0346.

***N*-(4-bromobutyl)-*N*-acetoxyacetamide 6**: To *N*-acetoxyacetamide **5** (400 mg, 3.4 mmol) solubilized in anhydrous DMF (16 mL) Cs_2CO_3 (2.2 g, 6.8 mmol) was added. The mixture was sonicated for 5 min. Dibromobutane (4 mL, 34 mmol) was added and the mixture was stirred at 100 °C for 2h under microwaves assistance. DMF was evaporated and CH_2Cl_2 (10 mL) was added, organic layer was washed twice with water. Organic layer was dried over Na_2SO_4 and evaporated. The crude was purified by flash chromatography on silica gel with cyclohexane/AcOEt (1/0 to 0/1) to afford **6** as colorless oil (300 mg, 35%). TLC Rf: 0.35 cyclohexane/AcOEt (2:8, v/v). ^{1}H NMR (500 MHz, $CDCl_3$) δ 4.16 (t, *J* = 6.3 Hz, 2H, $N\underline{CH_2}CH_2$), 3.43 (t, *J* = 6.7 Hz, 2H, $CH_2\underline{CH_2}Br$), 2.14 (s, 3H, $OC\underline{CH_3}$), 2.03 (s, 3H, $NOC\underline{CH_3}$), 2.00 – 1.94 (m, 2H, $\underline{CH_2}CH_2Br$), 1.89 – 1.82 (m, 2H, $NCH_2\underline{CH_2}$). ^{13}C NMR (101 MHz, $CDCl_3$) δ 168.8, 168.5, 66.8, 33.2, 29.4, 27.4, 19.7, 15.0. HR-ESI-QToF MS (positive mode): m/z calcd for $C_8H_{14}NO_3BrNa$ $[M+Na]^+$ 274.0055, found 274.0055.

***N*-(4-azidobutyl)-*N*-acetoxyacetamide 7:** *N*-(4-bromobutyl)-*N*-acetoxyacetamide **6** (88 mg, 0.35 mmol) was coevaporated twice with anhydrous CH_3CN. The residue was solubilized in anhydrous CH_3CN (2 mL) and tetramethylguanidinium azide (TMG N_3) (111 mg, 0.7 mmol) was added. The mixture was stirred at 80 °C for 1h30 under microwaves. CH_3CN was evaporated and the residue was purified by flash chromatography on silica gel with cyclohexane/AcOEt (1/1 to 0/1) to afford **7** as a colorless oil (44 mg, 59%). TLC Rf: 0.19 cyclohexane/AcOEt (3:7 v/v), ^{1}H NMR (400 MHz, $CDCl_3$) δ 4.14 (t, *J* = 6.2 Hz, 2H, $N\underline{CH_2}CH_2$), 3.31 (t, *J* = 6.6 Hz, 2H, $CH_2\underline{CH_2}N_3$), 2.13 (s, 3H, $OC\underline{CH_3}$), 2.02 (s, 3H, $NOC\underline{CH_3}$), 1.80 – 1.72 (m, 1H, $NCH_2\underline{CH_2}$), 1.72 – 1.63 (m, 1H, $\underline{CH_2}CH_2N_3$). ^{13}C NMR (101 MHz, $CDCl_3$) δ 168.8, 168.4, 67.0, 51.1, 26.0, 25.6, 19.6, 14.9. HR-ESI-QToF MS (positive mode): m/z calcd for $C_8H_{14}N_4O_3Na$ $[M+Na]^+$ 37.0964, found 237.0963.

2-[(4,4'-Dimethoxytrityl)oxymethyl]-2-methylpropan-3-ol-yl Levulinate 9: 2-[(4,4'-Dimethoxytrityl)oxymethyl]-2-methylpropane-1,3-diol **8**[19] (DMTrTHME) (850 mg, 2.0 mmol) was dissolved into 10 mL of anhydrous dichloromethane. Then, 1,3-dicyclohexylcarbodiimide (413 mg, 2.0 mmol) and 4-(dimethy1amino)pyridine (25 mg, 0.2 mmol) were added. After cooling to 0 °C, levulinic acid (205 µL, 2.0 mmol) was added. The mixture was stirred at 0 °C for 3h and 5 mL methanol was added, followed by addition of hexane (10 mL). After filtration of DCU, the solution was concentrated. The residue was purified by chromatography on silica gel using ethyl acetate, cyclohexane, triethylamine from 2:7:1 to 5:5:1 v/v/v and compound **9** was obtained as viscous

syrup (689 mg, 66%). TLC Rf: 0.20 cyclohexane/EtOAc/Et_3N (5:4:1 v/v/v). ^{1}H NMR (400 MHz, $CDCl_3$) δ 7.49 (m, 2H, Ar), 7.38 (m, 4H, Ar), 7.34 (m, 2H, Ar), 7.26 (t, *J* = 7.4 Hz, 1H, Ar), 6.90 (d, *J* = 8.8 Hz, 4H, Ar), 4.24 (s, 2H, COO$\underline{CH_2}$), 3.83 (s, 6H, $\underline{CH_3}$O), 3.53 (s, 2H, DMTrO$\underline{CH_2}$), 3.13 (q, *J* = 9.2 Hz, 2H, C$\underline{CH_2}$), 2.76 (t, *J* = 6.4 Hz, 2H, $CH_3CO\underline{CH_2}$), 2.58 (t, *J* = 6.6 Hz, 2H, $\underline{CH_2}$COO), 2.21 (s, 3H, OC$\underline{CH_3}$), 0.98 (s, 3H, Me). ^{13}C NMR (100 MHz, $CDCl_3$) δ 206.6, 172.9, 158.4, 144.8, 135.8, 130.0, 128.0, 127.8, 126.8, 113.1, 86.1, 66.8, 66.5, 66.0, 55.1, 40.6, 37.9, 29.7, 27.9, 17.4. HR-ESI-QToF MS (positive mode): m/z calcd. for $C_{31}H_{36}O_7Na$ $[M+Na]^+$ 543.2359, found 543.2357.**2-[(4,4'-Dimethoxytrityl)oxymethyl]-2-methylpropan-3-ol-yl Levulinate (2-cyanoethyl-*N*,*N*-diisopropyl) phoshoramidite 10:** To a solution of 2-[(4,4'-dimethoxytrityl)oxymethyl]-2-methylpropan-3-ol-yl levulinate **9** (265 mg, 0.5 mmol) and DIEA (131 µL, 0.75 mmol) in anhydrous CH_2Cl_2 (6 mL) was added 2-cyanoethyl-*N*,*N*-diisopropylchloro phosphoramidite (123 µL, 0.55 mmol). The resulting mixture was stirred for 1.5h at room temperature. Water (1 mL) was added and the solution was diluted with CH_2Cl_2 (15 mL), and washed with a saturated solution of $NaHCO_3$ (15 mL) then with brine (15 mL). The organic layer was dried over Na_2SO_4, filtered and concentrated. The crude product was purified by silica gel column chromatography using cyclohexane, AcOEt and triethylamine from 2:7:1 to 4:5:1, v/v/v affording **10** (307 mg, 85%) as clear oil. TLC Rf: 0.53 cyclohexane/AcOEt/NEt_3 (5:4:1 v/v/v). ^{1}H NMR (400 MHz, $CDCl_3$) δ 7.41 (m, 2H, Ar), 7.27 (m, 6H, Ar), 7.20 (m, 1H, Ar), 6.81 (m, 4H, Ar), 4.06 (m, 2H, COO$\underline{CH_2}$), 3.79 (s, 6H, $\underline{CH_3}$O), 3.71 (m, 2H, PO$\underline{CH_2}CH_2$), 3.52 (m, 4H, CH*i*Pr and DMTrO$\underline{CH_2}$), 3.01 (m, 2H, PO$\underline{CH_2}$C), 2.68 (m, 2H, CO$\underline{CH_2}$), 2.55 (m, 2H, $\underline{CH_2}$CN), 2.49 (m, 2H, $\underline{CH_2}$COO), 2.16 (s, 3H, $\underline{CH_3}$CO), 1.16 (d, *J* = 6.8 Hz, 6H, $\underline{CH_3}$CH), 1.16 (d, *J* = 6.8 Hz, 6H, $\underline{CH_3}$CH), 0.98 (d, *J*= 8.4 Hz, 3H, $\underline{CH_3}$C). ^{13}C NMR (100 MHz, $CDCl_3$) δ 206.6, 172.6, 158.5, 145.1, 136.2, 130.3, 128.4, 127.8, 126.8, 117.8, 113.1, 85.8, 66.8, 66.1, 64.8, 58.3, 55.3, 43.1, 40.6, 38.0, 30.0, 28.0, 24.7, 20.5, 17.1. ^{31}P NMR (121 MHz, $CDCl_3$) δ 148.0, 147.90. HR-ESI-QToF MS (positive mode): m/z calcd. for $C_{40}H_{56}N_2O_9P$ $[M+H_3O]^+$ 739.3723, found 739.3726.

Solid phase synthesis of Cy3-galactocluster siderophore derivatives

General procedure for immobilization on azide solid support 11 of propargyl α-D-mannoside 12 by CuAAC: An aqueous solution of propargyl mannoside (0.2M, 300 µL, 60 µmol), freshly prepared aqueous solutions of $CuSO_4$ (0.04M, 250 µL, 10 µmol) and sodium ascorbate (0.1M, 500 µL, 50 µmol), THPTA (0.1M, 300 µL, 30 µmol) and TEAAc buffer (2M, 500 µL) were added to 10 µmol of azide solid support **11**. The mixture was stirred at room temperature for 2h. The solution was removed, and CPG beads were washed with H_2O (10 mL), MeOH (10 mL), and CH_2Cl_2 (10 mL) and dried.

General procedure for incorporation of EG_2propargyl phosphoramidite 14: The solid-supported mannoside **13** (1 μmol) was treated by phosphoramidite chemistry, on a DNA synthesizer (ABI 394), with EG_2propargyl phosphoramidite **14**. Only coupling and oxidation steps were performed. For the coupling step, benzylmercaptotetrazole was used as an activator (0.3M in anhydrous CH_3CN) and EG_2Propargyl phosphoramidite (0.2M in anhydrous CH_3CN) was introduced three times with a 180s coupling time. Oxidation was performed with 0.1M commercial solution of iodide (0.1M in THF/pyridine/H_2O, 78:20:2, v/v/v) for 15s.

General procedure for phosphoramidite chemistry: Solid-supported (propagylEG_2)4-mannoside (1 μmol) was treated by phosphoramidite chemistry, on a DNA synthesizer. Detritylation step was performed with 3% TCA in CH_2Cl_2 for 65s. For the coupling step, benzylmercaptotetrazole (0.3M in anhydrous CH_3CN) was used with THME monolevulinyl **10**, THME monopropargyl **22a**, pentaerythritol dipropargyl **22b**, pentaerythritol tripropargyl **19** phosphoramidite (0.1M in anhydrous CH_3CN) with a 60s coupling time and Cy3 amidite (0.1M in anhydrous CH_3CN) with a 180s coupling time. The capping step was performed with commercial solution acetic anhydride (Cap A, Ac_2O/pyridine/THF, 5:10:85, v/v/v; Cap B, 10% *N*-methylimidazole in THF) for 10s. Oxidation was performed with 0.1M commercial solution of iodide for 15s. Synthesis was performed with Trityl ON mode.

General procedure for delevulinylation: The CPG beads were treated with a solution of 0.5M hydrazinium acetate (H_2NNH_2-H_2O/pyridine/AcOH, 0.124:4:1, v/v/v) for 30min, washed with pyridine, acetonitrile and CH_2Cl_2, and dried.

General procedure for introduction of galactoside azide derivative by CuAAC on solid support: In the column synthesis (1 μmol) were added the acetylated galactoside azide derivative **17** (0.1M in dioxane, 80 μL, 8 μmol), THPTA (0.1M in H_2O, 30 μL, 30 μmol), dioxane (20 μL) and a freshly prepared aqueous solutions of $CuSO_4$ (0.04M, 25 μL, 0.4 μmol) and sodium ascorbate (0.1M, 50 μL, 5 μmol), DNA column was vortexed at 60 °C in oven for 3h. The CPG beads were washed with dioxane, H_2O, MeOH, CH_2Cl_2 and dried under vacuum.

General procedure for deprotection and release from solid support: The CPG beads were transferred to a 4 mL screw top vial and treated with 2 mL of concentrated aqueous ammonia at room temperature overnight. The supernatant was withdrawn and evaporated. Crude was purified by C_{18} reversed phase HPLC. Pure product was co-evaporated several times with H_2O and then lyophilized.

General procedure for introduction of catechol or hydroxamate azide by CuAAC in solution: To a solution of Cy3 alkyne-galactocluster (1 mM in H_2O, 200 µL, 200 nmol) were added siderophore azide **3** or **7** (0.1M in dioxane, 2 eq/alkyne), THPTA (0.1M in H_2O, 6 µL, 600 nmol), dioxane (140 µL) and copper nanopowder (~ 1 mg). The mixture was stirred at room temperature for 2h, then after centrifugation, the supernatant was treated with EDTA solution (complete to 1 mL) and the mixture was purified two times by steric exclusion column (NAP 10). The conjugate was lyophilized in H_2O and acetyl groups were hydrolyzed by NEt_3/MeOH/H_2O (700 µL, 1:5:1, v/v/v) under stirring for 2h at room temperature. The siderophore-glycocluster conjugate was obtained after several co-evaporations with water and lyophilization from water.

2,3-Dibenzoxybenzoic acid 24: 2,3-Dihydroxybenzoic acid (100 mg, 0.6 mmol) was solubilized in pyridine (4 mL). Benzoic anhydride (440 mg, 1.9 mmol) was added and the reaction mixture was stirred at room temperature overnight. MeOH (6 mL) was added and solvent evaporated under vacuum. The residue was purified on flash silica gel chromatography with cyclohexane and AcOEt (1:0 to 0:1 v/v) to afford **24** as a colorless oil (201 mg, 93%). TLC Rf: 0.23 cyclohexane/AcOEt (3:7, v/v). ^{1}H NMR (400 MHz, $CDCl_3$) δ 8.08 – 8.00 (m, 5H, Ar), 7.62 (dd, *J* = 8.0, 1.5 Hz, 1H, Ar), 7.57 – 7.48 (m, 2H, Ar), 7.43 (t, *J* = 8.0 Hz, 1H, Ar), 7.39 – 7.31 (m, 4H, Ar). ^{13}C NMR (101 MHz, $CDCl_3$) δ 168.3, 164.4, 164.3, 144.2, 143.5, 134.0, 133.7, 130.5, 130.4, 130.4, 129.7, 128.7, 128.7, 128.6, 126.4. HR-ESI-QToF MS (negative mode): m/z calcd for $C_{21}H_{13}O_6$ $[M - H]^-$ 361.07176, found 361.07025

***N*-(3-Azidopropyl)-2,3-dibenzoxybenzamide 25:** To a cold solution (~ -10 °C) of **24** (2.2 g, 6 mmol) in dry CH_2Cl_2 (60 mL) and DIEA (2.1 mL, 12 mmol) was added dropwise ethyl chloroformate (914 µL, 9.6 mmol). After 15min stirring at -10 °C, azidopropylamine (901 mg, 9 mmol) and DIEA (1.05 mL, 6 mmol) were added. 15min after addition the solution was allowed to warm up to room temperature and stirred for 1h then the solution was applied on a silica gel column and chromatographed using an increasing amount of AcOEt (0 to 80%) in cyclohexane to obtain compound **25** (white solid, 1.8 g, 67%). TLC Rf: 0.54 cyclohexane/AcOEt (4:6, v/v). ^{1}H NMR (400 MHz, $CDCl_3$) δ 8.06 (dd, *J* = 8.3, 1.2 Hz, 2H, Ar), 7.99 (dd, *J* = 8.3, 1.2 Hz, 2H, Ar), 7.75 (dd, *J* = 7.7, 1.7 Hz, 1H, Ar), 7.60 – 7.52 (m, 1H, Ar), 7.52 – 7.48 (m, 2H, Ar), 7.45 – 7.36 (m, 3H, Ar), 7.33 (t, *J* = 7.9 Hz, 2H, Ar), 6.49 (t, *J* = 4.8 Hz, 1H, NH), 3.40 (dd, *J* = 12.7, 6.7 Hz, 2H, N$\underline{CH_2}CH_2$), 3.21 (t, *J* = 6.7 Hz, 2H, $CH_2\underline{CH_2}N_3$), 1.66 (p, *J* = 6.7 Hz, 2H, $NCH_2\underline{CH_2}CH_2N_3$). ^{13}C NMR (101 MHz, $CDCl_3$) δ 165.2, 164.4, 164.2, 143.3, 140.4, 134.4, 133.9, 130.9, 130.3, 130.2,

128.9, 128.6, 128.5, 128.1, 127.2, 127.0, 126.1, 49.2, 37.5, 28.8. HR-ESI-QToF MS (positive mode): m/z calcd for $C_{24}H_{21}N_4O_5$ $[M + H]^+$ 445.1512, found 445.1519

Triazolyl-catecholamide mannopyranoside 27: The propargyl-diethyleneglycol mannopyranoside **26** (520 mg, 1.7 mmol) was solubilized in dioxane/H_2O (3:1 v/v, 17 mL) and *N*-(3-azidopropyl)-2,3-dibenzoxybenzamide **25** (978 mg, 2.2 mmol), copper nanopowder (~ 4 mg) and TEAAc (2M, 500 µL) were added. The mixture was stirred at 55 °C overnight. Solvent was evaporated under vacuum and the crude was purified by silica gel flash chromatography (CH_2Cl_2/MeOH, 75:15 v/v). Product was treated with Quadrapure® IDA for 6h. The mixture was filtered and filtrate evaporated under vacuum. The residue was solubilized in a minimum of dioxane for lyophilization to obtain **27** as a white solid (1.11 g, 87%). TLC Rf: 0.15 CH_2Cl_2/MeOH (9:1, v/v). ^{1}H NMR (400 MHz, $CDCl_3$) δ 8.05 – 7.94 (m, 4H, Ar), 7.64 (s, 1H, Tz), 1H, 7.59 (d, *J* = 8.1 Hz, 1H, Ar), 7.55 – 7.47 (m, 2H, Ar), 7.43 (dd, *J* = 8.1 , 1.3 Hz, 1H, Ar), 7.37 – 7.28 (m, 5H, Ar), 7.24 (t, *J* = 5.6 Hz, 1H, NH), 4.89 (s, 1H, OH), 4.84 (s, 1H, H_1'), 4.75 (s, 1H, OH), 4.57 (s, 2H, O$\underline{CH_2}$Tz), 4.25 (t, *J* = 6.5 Hz, 2H, Tz$\underline{CH_2}CH_2$), 3.93 – 3.76 (m, 4H, H_2',H_4',H_{6a}',H_3'), 3.76 – 3.66 (m, 2H, H_{6b}', O$\underline{CH}$HCH_2), 3.66 – 3.49 (m, 8H, OCH$\underline{H}$CH_2, OCH_2, H_5'), 3.27 (dd, *J* = 11.5, 5.6 Hz, 2H, N$\underline{CH_2}CH_2$), 2.34 (s, 1H, OH), 1.98 – 1.88 (m, 2H, NC$H_2\underline{CH_2}CH_2$Tz). ^{13}C NMR (126 MHz, $CDCl_3$) δ 166.0, 164.4, 164.4, 144.8, 143.4, 140.5, 134.3, 134.1, 131.0, 130.3, 130.3, 128.9, 128.7, 128.4, 128.2, 126.9, 126.6, 126.0, 123.8, 100.2, 72.4, 71.6, 70.9, 70.7, 70.3, 69.8, 67.0, 66.7, 64.5, 61.4, 47.6, 36.8, 30.1. HR-ESI-QToF MS (positive mode): m/z calcd for $C_{37}H_{43}N_4O_{13}$ $[M + H]^+$ 751.2821, found 751.2848.

Mannopyranoside mono-catechol 28: To triazolyl-catecholamide mannopyranoside **27** (232 mg, 0.3 mmol) in anhydrous CH_3CN (1.5 mL), propargyldiethyleneglycol phosphoramidite **14** (707 mg, 2 mmol) was added and mixture was dried over molecular sieve 3Å for 1h. A solution of tetrazole (0.4M, 7.5 mL, 3 mmol) was added and the mixture was stirred at room temperature for 4h. Water (1 mL) was added and after 5min Amberlyst ® A26 IO_4^- resin (2.49 mmol/g, 1.2 g, 3 mmol) was added, the mixture was stirred for 2h. After filtration and dilution in CH_2Cl_2, the organic layer was washed with saturated solution of $NaHCO_3$ and brine. Organic layer was dried over Na_2SO_4 and solvent was evaporated under vacuum to afford crude **28** (yellow oil, 614 mg, quantitative) which was used for the next step without further purification. TLC Rf: 0.22 CH_2Cl_2/MeOH (95:5, v/v). ^{1}H NMR (400 MHz, CD_3CN) δ 8.03 – 7.95 (m, 4H, Ar), 7.69 (s, 1H, Tz), 7.65 – 7.58 (m, 3H, Ar), 7.55 (dd, *J* = 8.1, 1.8 Hz, 1H, Ar), 7.52 – 7.38 (m, 5H, Ar), 7.15 (t, *J* = 6.1 Hz, 1H, NH), 5.16 – 5.07 (m, 1H, H_1'), 4.86 – 4.79 (m, 1H, H_3'), 4.75 – 4.51 (m, 5H, H_4', H_2', OCH_2Tz), 4.42 – 3.75 (m, 40H, OCH_2, $\underline{CH_2}$Tz, $\underline{CH_2}CH_2CN$, PO$\underline{CH_2}$, $\underline{CH_2}$CCH, H_5'), 3.75 – 3.44 (m, 44H, H_6', OCH_2), 3.26 (m, 2H, N$\underline{CH_2}CH_2$), 2.91 – 2.76 (m, 8H, $CH_2\underline{CH_2}$CN), 2.71 (t, *J* = 3.6 Hz, 4H, $CH_2C\underline{CH}$), 2.01 (p, *J* =

6.8 Hz, 2H, $NCH_2\underline{CH_2}CH_2Tz$). ^{13}C NMR (101 MHz, CD_3CN) δ 166.0, 165.2, 164.9, 145.3, 144.4, 141.4, 135.1, 135.1, 132.5, 130.9, 130.8, 129.8, 129.8, 129.5, 129.3, 127.8, 127.3, 126.7, 124.5, 118.7, 98.2, 80.9, 75.8, 75.6, 75.0, 71.8, 71.1, 70.9, 70.5, 69.9, 68.73, 68.4, 68.3, 66.6, 64.8, 63.9, 63.4, 58.7, 48.3, 37.4, 30.8, 20.2. ^{31}P NMR (162 MHz, CD_3CN) δ -1.69, -1.74, -2.18, -2.35 (PO), -2.42, -2.66, -2.73 (POO-). HR-ESI-QToF MS (positive mode): m/z calcd for $C_{77}H_{99}N_8O_{33}P_4$ $[M + H]^+$ 1787.5265, found 1787.5258.

Galactocluster mono-catechol G1C: Tetra-propargyl mannopyranoside mono-catechol **28** (536 mg, 0.3 mmol) was solubilized in dioxane /H_2O (1:1 v/v, C = 0.05M, 6 mL) and acetylated galacto-azide derivative **17a** (784 mg, 1.5 mmol) was added followed by copper nanopowder (~ 2 mg) and TEAAc (2M, 1 mL). Mixture was stirred at 55 °C for 24h (the reaction was monitored by MALDI-TOF spectrometry). The crude was purified by silica gel flash chromatography (CH_2Cl_2/MeOH, 85:15 v/v) to obtain protected galactocluster mono-catechol (yellow solid, 863 mg, 74%) after treatment with Quadrapure® IDA (500 mg) overnight. Solution was filtered and filtrate lyophilized. ^1H NMR (400 MHz, CD_3CN) δ 9.02 (s, 4H, NH), 8.00 – 7.94 (m, 4H, Ar), 7.92 – 7.80 (m, 4H, Tz), 7.69 (s, 1H, Tz), 7.64 – 7.32 (m, 17H, Ar), 7.25 (s, 1H, NH), 6 .97 (d, *J* = 8.9 Hz, 8H, Ar), 5.44 – 5.37 (m, 4H, H_4'gal), 5.31 – 5.06 (m, 25H, H_2'gal, H_3'gal, $OCCH_2Tz$, H_1'gal, H_1'man), 4.87 – 4.80 (m, 1H, H_2'man), 4.73 – 4.63 (m, 1H, H_3'man), 4.63 – 4.44 (m, 11H, OCH_2Tz, H_4'man), 4.32 – 4.00 (m, 38H, $Tz\underline{CH_2}CH_2$, $\underline{CH_2}CH_2CN$, $OP\underline{CH_2}CH_2$, H_6'gal, H_5'gal, H_6'man, H-$_5$'man), 3.68 – 3.46 (m, 49H, OCH_2), 3.24 (q, *J* = 6.1 Hz, 2H, $N\underline{CH_2}CH_2$), 2.85 – 2.70 (m, 8H, $CH_2\underline{CH_2}CN$), 2.19 – 2.08 (m, 14H, $NCH_2\underline{CH_2}CH_2Tz$, $OC\underline{CH_3}$), 2.02 (s, 12H, $OC\underline{CH_3}$), 1.97 (s, 12H, $OC\underline{CH_3}$), 1.94 (s, 12H, $OC\underline{CH_3}$). ^{13}C NMR (101 MHz, CD_3CN) δ 171.2, 171.1, 170.8, 170.5, 165.1, 154.5, 145.6, 135.1, 134.5, 130.8, 129.8, 127.8, 127.3, 126.2, 122.3, 118.7, 100.3, 72.0, 71.5, 71.1, 70.3, 69.6, 68.3, 67.7, 64.8, 64.0, 62.3, 53.4, 48.4, 37.5, 30.8, 20.9, 20.2. ^{31}P NMR (202 MHz, $CDCl_3$) δ -2.70 (PO). MALDI-TOF MS (negative mode, THAP): m/z calcd for $C_{165}H_{201}N_{24}O_{77}P_4Na$ $[M – 2H + Na]^-$ 3899.40, found 3900.25, for $C_{162}H_{198}N_{23}O_{77}P_4$ $[(M – Cne) - H]^-$ 3823.35, found 3822.20. HR-ESI-QToF MS (positive mode): m/z calcd for $C_{165}H_{204}N_{24}O_{77}P_4$ $[(M + 2H)/2]^+$ 1938.5868, found 1938.5840.

The protected galactocluster mono-catechol (0.15 mmol, 595 mg) was stirred at room temperature overnight in NEt_3/MeOH/H_2O (1:5:1 v/v/v, 21 mL). Solvents were evaporated under vacuum. The crude was purified on reverse phase flash chromatography (H_2O/1% CH_3CN 25 mM TEAAc - H_2O/20% CH_3CN 25 mM TEAAc). Triethylammonium ion were exchanged to Na^+ by treatment with DOWEX® 50W X8 Na+ form resin. The product was lyophilized in H_2O to give galactocluster mono-catechol **G1C** (beige solid, 321 mg, 74%). ^1H NMR (400 MHz, D_2O) δ 8.18 –

7.75 (m, 5H, Tz), 7.42 – 7.24 (m, 8H, Ar), 7.11 – 6.88 (m, 11H, Ar), 6.86 – 6.60 (m, 1H, NH), 5.48 – 5.16 (m, 8H, $OCCH_2Tz$), 5.16 – 5.05 (m, 1H, H_1'man), 5.02 – 4.88 (m, 5H, sugar), 4.73 – 4.25 (m, 21H, $OPCH_2$, OCH_2Tz, sugar), 4.20 – 3.40 (m, 88H, OCH_2, sugar), 3.40 – 3.30 (m, 2H, $N\underline{CH_2}CH_2$), 2.23 – 2.08 (m, 2H, $NCH_2\underline{CH_2}CH_2Tz$). ^{13}C NMR (101 MHz, D_2O) δ 181.5, 165.8, 154.2, 144.1, 131.4, 126.5, 123.1, 117.0, 101.0, 75.3, 72.5, 70.5, 70.3, 69.5, 68.9, 68.5, 64.9, 63.1, 60.7, 52.4, 23.3. ^{31}P NMR (162 MHz, D_2O) δ 0.69, -0.60, -0.85 (PO). C18 HPLC (1% to 24% CH_3CN 50 mM TEAAc over 20min): Rt= 13.2 min. MALDI-TOF MS (negative mode, THAP): m/z calcd for $C_{107}H_{149}N_{20}O_{59}P_4$ $[M-H]^-$ 2783.34, found 2783.22, and calcd for $C_{107}H_{149}N_{20}O_{59}P_4Na$ $[M - 2H + Na]^-$ 2805.33, found 2805.18. HR-ESI-QToF MS (positive mode): m/z $C_{107}H_{152}N_{20}O_{59}P_4$ calcd for $[(M+2H)/2]^+$ 1392.4230, found 1392.4210 and calcd for $C_{107}H_{153}N_{20}O_{59}P_4$ $[(M+3H)/3]^+$ 928.6179, found 928.6185.

Triazolyl-diethyleneglycol galactopyranoside 29: Propargyl diethyleneglycol (1 mmol, 144.2 mg) was solubilized in dioxane/H_2O (5:1 v/v, 12 mL) and galactoside azide derivative **17a** (1 mmol, 522 mg) was added followed by copper nanopowder (0.016 mmol, 1 mg) and TEAAc (2M, 200 µL). The mixture was stirred at 55 °C overnight. Solvent was evaporated under vacuum and the crude was purified on silica gel flash chromatography (CH_2Cl_2/MeOH, 95:5 v/v) to obtain **29** (white solid, 545 mg, 82%). TLC Rf: 0.2 (CH_2Cl_2/MeOH, 9:1 v/v). ^1H NMR (400 MHz, $CDCl_3$) δ 8.61 (s, 1H, NH), 7.81 (s, 1H, Tz), 7.41 (d, *J* = 8.9 Hz, 2H, Ar), 6.94 (d, *J* = 8.9 Hz, 2H, Ar), 5.50 – 5.39 (m, 2H, H_2', H_4'), 5.18 (s, 2H, $OC\underline{CH_2}Tz$), 5.10 (dd, *J* = 10.5, 3.4 Hz, 1H, H_3'), 4.99 (d, *J* = 7.9 Hz, 1H, H_1'), 4.70 (s, 2H, $O\underline{CH_2}Tz$), 4.21 (dd, *J* = 11.3, 7.0 Hz, 1H, H_{6a}'), 4.14 (dd, *J* = 11.3, 6.2 Hz, 1H, H_{6b}'), 4.04 (t, *J* = 6.7 Hz, 1H, H_5'), 3.79 – 3.65 (m, 6H, OCH_2), 3.65 – 3.52 (m, 2H, OCH_2), 3.04 (s, 1H, OH), 2.17 (s, 3H, $OCCH_3$), 2.06 (s, 3H, $OCCH_3$), 2.04 (s, 3H, $OCCH_3$), 2.00 (s, 3H, $OCCH_3$). ^{13}C NMR (101 MHz, $CDCl_3$) δ 170.5, 170.4, 170.3, 169.6, 163.4, 154.1, 145.5, 132.7, 125.1, 122.0, 117.7, 100.1, 72.6, 71.2, 71.0, 70.5, 70.1, 68.8, 67.0, 64.5, 61.7, 61.5, 53.6, 20.9, 20.8, 20.8, 20.7. HR-ESI-QToF MS (positive mode): m/z calcd for $C_{29}H_{39}N_4O_{14}$ $[M + H]^+$ 667.2457, found 667.2461.

Triazolyl-diethyleneglycol galactopyranoside phosphoramidite 30: The galactoside derivative **29** (3.36 mmol, 2.24 g) was co-evaporated twice with anhydrous CH_3CN, and product was solubilized in anhydrous CH_2Cl_2 (45 mL). Anhydrous DIEA (4.7 mmol, 820 µL) was added and mixture was dried over molecular sieve (4 Å) for 2h under argon atmosphere and $CaCl_2$ guard. At 0 °C, cyanoethyl-*N*,*N*-diisopropyl phosphoramidite chloride (3.7 mmol, 875 µL) was added dropwise and the mixture was stirred for 1h at room temperature. H_2O (1 mL) was added, after 5min organic layer was washed twice with a saturated solution of $NaHCO_3$. Organic layer was dried over Na_2SO_4

and solvent evaporated under vacuum. The residue was purified on silica gel flash chromatography (CH_2Cl_2/AcOEt/10% NEt_3, 9:1 v/v 10% NEt_3) to obtain phosphoramidite **30** (white solid, 2.28 g, 78%). TLC Rf: 0.2 (CH_2Cl_2/AcOEt/10% NEt_3, 7:2, v/v 10% NEt_3). ^{1}H NMR (400 MHz, $CDCl_3$) δ 8.45 (s, 1H, NH), 7.80 (s, 1H, Tz), 7.41 (d, *J* = 9.0 Hz, 2H, Ar), 6.94 (d, *J* = 9.0 Hz, 2H, Tz), 5.51 – 5.40 (m, 2H, H_2', H_4'), 5.17 (s, 2H, OC$\underline{CH_2}$Tz), 5.09 (dd, *J* = 10.5, 3.4 Hz, 1H, H_3'), 4.98 (d, *J* = 8.0 Hz, 1H, H_1'), 4.70 (s, 2H, O$\underline{CH_2}$Tz), 4.27 – 4.10 (m, 2H, H_6'), 4.04 (t, *J* = 6.9 Hz, 1H, H_5'), 3.89 – 3.75 (m, 2H, PO$\underline{CH_2}CH_2CN$), 3.75 – 3.62 (m, 8H, OCH_2), 3.62 – 3.50 (m, 2H, N$\underline{CH}$), 2.62 (t, *J* = 6.0 Hz, 2H, $POCH_2\underline{CH_2}CN$), 2.16 (s, 3H, $OCCH_3$), 2.05 (s, 3H, $OCCH_3$), 2.04 (s, 3H, $OCCH_3$), 2.00 (s, 3H, $OCCH_3$), 1.16 (d, *J* = 6.7 Hz, 6H, NCH$\underline{CH_3}$), 1.14 (d, *J* = 6.7 Hz, 6H, $NCHCH_3$). ^{13}C NMR (101 MHz, $CDCl_3$) δ 170.5, 170.5, 170.2, 169.5, 163.3, 154.1, 145.8, 132.6, 124.8, 121.9, 118.1, 117.7, 100.1, 71.4, 71.2, 70.9, 70.7, 70.1, 68.8, 67.0, 64.7, 62.8, 62.6, 61.5, 58.7, 58.5, 53.5, 43.2, 43.1, 24.8, 24.7, 24.7, 20.9, 20.8, 20.8, 20.7, 20.5, 20.4. ^{31}P NMR (162 MHz, $CDCl_3$) δ 148.51. HR-ESI-QToF MS (positive mode): m/z calcd for $C_{38}H_{56}N_6O_{15}P$ $[M + H]^+$ 867.3536, found = 867.3525.

Galactocluster diethyleneglycol 32: The propargyl-diethyleneglycol mannopyranoside **26** (92 mg, 0.3 mmol) and galactopyranoside phosphoramidite **30** (1.81 g, 2.1 mmol) were solubilized in dry CH_3CN (12 mL) and mixture was dried over molecular sieve 3Å for 1h. Then BMT (519 mg, 2.7 mmol) as activator was added and the mixture was stirred at room temperature for 4h. H_2O was added and after 5min, Amberlyst ® A26 IO_4^- resin (2.49 mmol/g, 1 g) was added, the mixture was stirred for 2h. After filtration, solvent was evaporated under vacuum (MALDI-TOF MS (positive mode, THAP): m/z calcd for $C_{141}H_{183}N_{20}O_{72}P_4$ $[M+H]^+$ 3433.98, found 3434.05). The crude product was treated with 30% ammonia for 2h at room temperature. After evaporation under vacuum, the residue was purified on reverse phase flash chromatography (H_2O/1% CH_3CN 25 mM TEAAc - 80% CH_3CN 25 mM TEAAc) and lyophilized in H_2O to afford product **32** (yellow solid, 409 mg, 54%). ^{1}H NMR (500 MHz, D_2O) δ 8.08 – 8.03 (m, 4H, Tz), 7.33 (d, *J* = 8.9 Hz, 8H, Ar), 7.04 (d, *J* = 7.7 Hz, 8H, Ar), 5.36 – 5.28 (m, 8H, OC$\underline{CH_2}$Tz), 5.01 (s, 1H, H_1'man), 4.92 (d, *J* = 7.6 Hz, 4H, H-$_1$'gal), 4.70 – 4.54 (m, 9H, O$\underline{CH_2}$Tz, H'man), 4.40 – 4.28 (m, 1H, H'man), 4.28 – 4.20 (m, 1H, H'man), 4.12 (d, *J* = 2.2 Hz, 2H, $\underline{CH_2}$CCH), 4.08 – 3.98 (m, 6H, PO$\underline{CH}$H, H'man), 4.00 – 3.90 (m, 7H, PO$\underline{CH}\underline{H}$, H'gal), 3.91 – 3.83 (m, 2H, H'man), 3.83 – 3.51 (m, 54H, H'gal, OCH_2), 2.81 (t, *J* = 2.2 Hz, 1H, $CH_2C\underline{CH}$). ^{13}C NMR (126 MHz, D_2O) δ 180.7, 165.1, 153.4, 143.4, 137.0, 130.5, 125.7, 122.4, 116.1, 100.1, 97.0, 78.6, 71.7, 69.7, 69.3, 68.7, 68.6, 68.1, 67.7, 67.6, 64.0, 63.9, 62.2, 59.8, 57.0, 51.6, 36.7. ^{31}P NMR (202 MHz, D_2O) δ 0.52, -0.74, -0.80, -0.97. HPLC C18 (1% to 24% CH_3CN 50 mM TEAAc over 20min): 11.8 min. MALDI-TOF MS (negative mode,

THAP): m/z calcd for $C_{97}H_{137}N_{16}O_{56}P_4$ $[M-H]^-$ 2547.11, found 2547.38. HR-ESI-QToF MS (positive mode): m/z calcd for $C_{97}H_{140}N_{16}O_{56}P_4$ $[(M + 2H)/2]^+$ 1274.3769, found 1274.3739.

Tosyl-triethyleneglycol 2-cyanotethyl diisopropyl phosphoramidite 34: To a solution of tosyl-triethyleneglycol[33] (460 mg 1.5 mmol) and DIEA (392 µL, 2.25 mmol) in anhydrous CH_2Cl_2 (25 mL) was added 2-cyanoethyl-*N*,*N*-diisopropylchloro phosphoramidite (334 µL, 1.5 mmol). The resulting mixture was stirred for 1h at room temperature. Water (1 mL) was added and the solution was diluted with CH_2Cl_2 (40 mL), and washed with a saturated solution of $NaHCO_3$ (40 mL) then with brine (42 mL). The organic layer was dried (Na_2SO_4), filtered, and concentrated. The crude product was purified by silica gel column chromatography using cyclohexane and ethyl acetate 90:10 to 70:30 v/v with 4% of triethylamine affording tosyl-triethyleneglycol phosphoramidite **34** (486 mg, 64%) as a colorless oil. ^{1}H-NMR ($CDCl_3$, 300 MHz) δ 7.80 (d, 2H, *J* = 8.3Hz, Ar), 7.34 (d, 2H, *J* = 8.2Hz, Ar), 4.2-4.18 – 4.09 (m, 2H, TosO$\underline{CH_2}$), 3.91 - 3.44 (m, 14H, N$\underline{CH}$, PO$\underline{CH_2}CH_2CN$, OCH_2), 2.64 (t, 2H, *J* = 6.5Hz, $POCH_2\underline{CH_2}CN$), 2.45 (s, 3H, Ph$\underline{CH_3}$), 1.18 (d, 6H, *J* = 6.5Hz, CH$\underline{CH_3}$), 1.17 (d, 6H, *J* = 6.5Hz, CH$\underline{CH_3}$). ^{13}C-NMR ($CDCl_3$, 101 MHz): δ 145.0, 133.1, 130.0, 128.1, 118.0, 71.4, 71.4, 71.0, 70.7, 69.4, 68.8, 62.8, 62.6, 58.7, 58.5, 53.6, 43.2, 43.1, 24.8, 24.7, 24.8, 21.8, 20.5, 20.4. ^{31}P-NMR ($CDCl_3$, 121 MHz): δ 148.7 ppm. HR-ESI-QToF MS (positive mode): m/z calcd for $C_{22}H_{40}N_2O_8PS$ $[M+H_3O]^+$ 523.2243, found 523.2223.

Tripropargyl-pentaerythrityl tosyl-triethyleneglycol cyanoethyl phosphate 35: To tripropargyl pentaerythritol **33** (112 mg, 0.45 mmol) in anhydrous CH_3CN (2 mL), tosyl-triethyleneglycol phosphoramidite **34** (297 mg, 0.6 mmol) was added and mixture was dried over molecular sieve 3Å for 1h. A solution of tetrazole (0.4M, 3 mL, 1.2 mmol) was added and the mixture was stirred at room temperature for 2h. Water was added (1 mL) and after 5 min Amberlyst ® A26 IO_4^- resin (2.49 mmol/g, 482 mg, 1.2 mmol) was added, the mixture was stirred for 2h. After filtration and dilution in CH_2Cl_2, the organic layer was washed with saturated solution of $NaHCO_3$ and brine. Organic layer was dried over Na_2SO_4 and solvent was evaporated under vacuum. Crude was purified on silica gel flash chromatography (CH_2Cl_2/MeOH, 95:5 v/v) to obtain **35** (yellow oil, 176 mg, 59%). TLC Rf: 0.43 (CH_2Cl_2/MeOH, 95:5, v/v). ^{1}H NMR (600 MHz, $CDCl_3$) δ 7.80 (d, *J* = 8.3 Hz, 2H, Ar), 7.35 (d, *J* = 8.0 Hz, 2H, Ar), 4.32 – 4.18 (m, 4H, PO$\underline{CH_2}CH_2CN$, PO$\underline{CH_2}$), 4.18 – 4.06 (m, 10H, TosO$\underline{CH_2}$, PO$\underline{CH_2}$C, O$\underline{CH_2}$CCH), 3.72 – 3.67 (m, 4H, OCH_2), 3.63 – 3.58 (m, 4H, OCH_2), 3.53 (s, 6H, C$\underline{CH_2}$O), 2.79 (t, *J* = 6.4 Hz, 2H, $POCH_2\underline{CH_2}CN$), 2.45 (s, 3H, $PhCH_3$), 2.43 (t, *J* = 2.4 Hz, 3H, $CH_2C\underline{CH}$). ^{13}C NMR (151 MHz, $CDCl_3$) δ 145.0, 133.1, 130.0, 128.1, 116.8, 79.8, 74.6, 70.9, 70.7, 69.4, 69.0, 68.3, 67.3, 67.2, 62.0, 58.9, 45.0, 44.9, 21.8, 19.7. ^{31}P NMR (162 MHz,

$CDCl_3$) δ -1.78. HR-ESI-QToF MS (positive mode): m/z calcd for $C_{30}H_{41}NO_{12}PS$ $[M + H]^+$ 670.2082, found 670.2077.

[Tri-(2,3-dibenzoxybenzamide propyl triazol)-pentaerythrityl] tosyl-triethyleneglycol cyanoethyl phosphate 36: Compound **35** (1.17 g, 1.7 mmol) was solubilized in dioxane/H_2O (3:1 v/v, 17 mL) and *N*-(3-azidopropyl)-2,3-dibenzoxybenzamide **25** (3.02 g, 6.8 mmol), copper (4 mg, 0.068 mmol) and TEAAc (2M, 500 µL) were added. The mixture was stirred at 55 °C overnight. After filtration and evaporation, the residue was solubilized in a minimum of CH_3CN and treated with Quadrapure® IDA (500 mg) for 3h. The mixture was filtered and filtrate evaporated. The crude was purified on silica gel flash chromatography (CH_2Cl_2/MeOH, 95:5 v/v). Residue was solubilized in a minimum of dioxane for lyophilization to obtain **36** (white solid, 2.21 g, 65%). TLC Rf: 0.21 (CH_2Cl_2/MeOH, 95:5 v/v). ^{1}H NMR (400 MHz, $CDCl_3$) δ 8.05 – 7.94 (m, 12H, Ar), 7.75 (d, *J* = 8.3 Hz, 2H, Ar), 7.67 (s, 3H, Tz), 7.58 (dd, *J* = 7.8, 1.6 Hz, 3H, Ar), 7.55 – 7.48 (m, 6H, Ar), 7.44 – 7.39 (m, 3H, Ar), 7.38 – 7.27 (m, 17H, Ar), 7.21 (t, *J* = 5.9 Hz, 3H, NH), 4.53 (s, 6H, O$\underline{CH_2}$Tz), 4.26 (t, *J* = 6.7 Hz, 6H, Tz$\underline{CH_2}CH_2$), 4.15 – 3.97 (m, 8H, PO$\underline{CH_2}$, TosO$\underline{CH_2}$, PO$\underline{CH_2}CH_2$, PO$\underline{CH_2}$C), 3.66 – 3.58 (m, 4H, O$\underline{CH_2}$), 3.56 – 3.52 (m, 4H, O$\underline{CH_2}$), 3.44 (s, 6H, C$\underline{CH_2}$O), 3.28 (dd, *J* = 12.6, 6.2 Hz, 6H, $CH_2\underline{CH_2}$N), 2.72 – 2.63 (m, 2H, POCH$_2\underline{CH_2}$CN), 2.41 (s, 3H, Ph$\underline{CH_3}$), 2.04 – 1.92 (m, 6H, TzCH$_2\underline{CH_2}CH_2$N). ^{13}C NMR (101 MHz, $CDCl_3$) δ 165.9, 164.4, 164.3, 145.0, 143.5, 140.6, 134.2, 134.0, 133.0, 131.3, 130.3, 130.3, 130.1, 128.8, 128.7, 128.5, 128.3, 128.1, 126.7, 126.6, 125.9, 123.4, 117.3, 70.8, 70.5, 69.9, 69.5, 68.8, 68.3, 67.3, 65.0, 62.2, 47.5, 45.2, 36.8, 30.1, 21.8, 19.6. ^{31}P NMR (162 MHz, $CDCl_3$) δ -2.17, -2.21, -2.25. HR-ESI-QToF MS (positive mode): m/z calcd for $C_{102}H_{101}N_{13}O_{27}PS$ $[M + H]^+$ 2002.6388, found 2002.6431, m/z calcd for $C_{102}H_{102}N_{13}O_{27}PS$ $[(M + 2H)/2]^+$ 1001.8233, found 1001.8260, m/z calcd for $C_{102}H_{103}N_{13}O_{27}PS$ $[(M + 3H)/3]^+$ 668.2181, found 668.2202.

[Tri-(2,3-dibenzoxybenzamide propyl triazol) pentaerythrityl] azido-triethyleneglycol phosphate 37: Compound **36** (1.93 g, 0.96 mmol) was solubilized in NEt_3/MeOH/H_2O mixture (1:5:1 v/v/v, 100 mL) and mixture was stirred at room temperature overnight. Reaction was monitored by MALDI-TOF spectrometry. Solvents were evaporated under vacuum and residue was solubilized in DMF (20 mL). $TMGN_3$ (184 mg, 1.16 mmol) was added and the solution was heated to 55 °C overnight. Solvent was evaporated and residue was solubilized in anhydrous pyridine (20 mL) and cooled to -5 °C then benzoyl chloride was added dropwise (744 µL, 6.4 mmol) and crude was stirred for 1h at 0 °C. Solvent was evaporated and residue was purified on reverse phase flash chromatography (H_2O/32% CH_3CN 50 mM TEAAc - 80% CH_3CN 25 mM TEAAc). Tampon was co-evaporated with H_2O and CH_3CN. Residue was lyophilized in dioxane to give **37** (white solid,

447 mg, 29%). ^{1}H NMR ($CDCl_3$, 400 MHz) δ 8.03 – 7.93 (m, 12 H, Ar), 7.84 (s, 3H, Tz), 7.67 – 7.60 (m, 3H, Ar), 7.55 – 7.46 (m, 6H, Ar), 7.43 – 7.37 (m, 3H, Ar), 7.37 – 7.28 (m, 15H, Ar), 4.58 – 4.50 (m, 6H, O$\underline{CH_2}$Tz), 4.33 – 4.21 (m, 6H, Tz$\underline{CH_2}CH_2$), 3.98 – 3.86 (m, 2H, PO$\underline{CH_2}$), 3.85 – 3.79 (m, 2H, $CH_2\underline{CH_2}N_3$), 3.65 – 3.54 (m, 8H, PO$\underline{CH_2}$C, OCH_2), 3.45 (s, 6H, C$\underline{CH_2}$O), 3.36 – 3.20 (m, 10H, $CH_2\underline{CH_2}$N, O$\underline{CH_2}$), 2.78 (q, *J* = 7.2 Hz, 12H, $\underline{CH_2}CH_3$ triethyl ammonium), 2.06 – 1.89 (m, 6H, Tz$CH_2\underline{CH_2}CH_2$N), 1.12 (t, *J* = 7.3 Hz, 18H, $CH_2\underline{CH_3}$ triethyl ammonium). ^{13}C NMR ($CDCl_3$, 101 MHz) δ 176.4, 166.3, 166.2, 164.4, 164.2, 145.0, 143.2, 140.4, 134.1, 134.0, 131.1, 130.3, 130.1, 128.8, 128.6, 128.2, 128.1, 126.6, 126.3, 125.6, 123.5, 70.4, 69.8, 68.6, 66.1, 64.4, 49.2, 49.0, 48.9, 48.7, 47.5, 45.2, 36.6, 36.5, 29.8, 22.2, 8.3, 8.2. ^{31}P NMR (202 MHz, $CDCl_3$) δ -0.26. C18 HPLC (32% to 80% CH_3CN in 50 mM TEAAc over 20min): 15min. MALDI-TOF MS (negative mode, THAP): m/z calcd for $C_{92}H_{89}N_{15}O_{24}P$ $[M - H]^-$ 1819.78, found 1819.76. HR-ESI-QToF MS (positive mode): m/z Calcd for $C_{92}H_{91}N_{15}O_{24}P$ $[M + H]^+$ 1820.6099, found 1820.6093, m/z calcd for $C_{92}H_{92}N_{15}O_{24}P$ $[(M + 2H)/2]^+$ 910.8088, found 910.8104.

Benzoylated galactocluster tri-catechol BzG3C: To a solution of galactocluster mannoside alkyne **32** (400 mg, 0.156 mmol) and tri-catechol platform **37** (312 mg, 0.172 mmol) in dioxane/H_2O (5:1 v/v, 12 mL) and TEAAc (2M, 60 µL), THPTA (68 mg, 0.156 mmol) and copper nanopowder (4 mg, 0.063 mmol) were added and stirred for 6 days. After filtration and evaporation, the crude dissolved in CH_3CN/H_2O, (1:1 v/v, 5mL) and was treated with Quadrapure® (800 mg) for 6h. The crude was purified on reverse phase by flash chromatography (H_2O/1% CH_3CN 25 mM TEAAc - 80% CH_3CN 25 mM TEAAc). The product was freeze-dried to afford compound **BzG3C** together with partially deprotected products. A pure fraction was isolated for characterization. HPLC C18 (1% to 24% CH_3CN 50 mM TEAAc over 12 min and 24% to 80% CH_3CN 50 mM TEAAc over 7 min): 17.5 min. ^{1}H NMR (600 MHz, D_2O) δ 8.12 – 7.96 (m, 8H, Tz, NH), 7.92 – 7.86 (m, 3H, Tz), 7.76 – 7.55 (m, 11H, Ar), 7.54 – 7.40 (m, 19H, Ar), 7.40 – 7.27 (m, 18H, Ar), 7.27 – 7.12 (m, 12H, Ar), 7.14 – 6.96 (m, 25H, Ar), 6.96 – 6.68 (m, 18H, Ar), 5.39 – 5.14 (m, 17H, OC$\underline{CH_2}$Tz), 5.10 (s, 3H, H_1'man), 4.98 – 4.89 (m, 11H, H_1'gal, H'man), 4.71 – 4.22 (m, 46H, C$\underline{CH_2}$Tz, $OCH_2\underline{CH_2}$Tz), 4.19 – 3.92 (m, 39H, $CH_2\underline{CH_2}$Tz, H'gal, PO$\underline{CH_2}$), 3.92 – 3.03 (m, 156H, OCH_2, H'gal, PO$\underline{CH_2}$C, C$\underline{CH_2}$O, N$\underline{CH_2}CH_2$), 1.88 – 1-60 (m, 6H, $NCH_2\underline{CH_2}CH_2$Tz). ^{13}C NMR (151 MHz, D_2O) δ 181.5, 175.8, 165.3, 154.2, 144.2, 136.3, 131.6, 131.2, 129.7, 128.8, 128.3, 127.4, 126.5, 123.0, 117.0, 101.0, 75.3, 72.6, 70.5, 69.5, 69.0, 68.4, 64.8, 64.7, 64.5, 63.7, 63.1, 60.7, 52.4, 49.8, 47.5, 46.6, 36.4, 29.1, 23.3. ^{31}P NMR (202 MHz, D_2O) δ 0.57, 0.34, -0.82, -1.02 (PO). MALDI-TOF MS (positive mode, THAP): m/z calcd for $C_{189}H_{229}N_{31}O_{80}P_5$ $[M+H]^+$ 4369.92, found 4370.49. MALDI-TOF MS (negative mode, THAP): m/z calcd for $C_{189}H_{227}N_{31}O_{80}P_5$ $[M-H]^-$ 4367.92, found 4367.0.

HR-ESI-QToF MS (positive mode): m/z calcd for $C_{189}H_{231}N_{31}O_{80}P_5$ $[(M + 3H)/3]^+$ 1456.4544, found 1456.4528.

Galactocluster tri-catechol G3C: A solution of the benzoylated galactocluster tricatechol **BzG3C** (~ 300 mg) in NEt_3/MeOH/H_2O (1:5:1 v/v/v, 30 mL) was kept at room temperature overnight, then extracted three times with AcOEt and triethyl ammonium was exchanged with Dowex 50 W X8 Na^+ to give after lyophilization **G3C** (brown solid, 220 mg, 37%, ~~for~~ two steps). ^{1}H NMR (600 MHz, D_2O) δ 8.22 – 7.75 (m, 8H, Tz), 7.51 – 6.73 (m, 19H, Ar), 5.39 (s, 8H, OC$\underline{CH_2}$Tz), 5.11 (s, 1H, H_1'man), 5.05 – 4.85 (m, 4H, H_1'gal), 4.75 – 4.24 (m, 29H, H'man, Tz$\underline{CH_2}$O, $CH_2\underline{CH_2}$Tz), 4.23 – 2.96 (m, 104H, PO$\underline{CH_2}$, PO$\underline{CH_2}$C, OCH_2, H'gal, H'man, N$\underline{CH_2}CH_2$) 2.31 – 1.94 (m, 6H, $NCH_2\underline{CH_2}CH_2$Tz). ^{13}C NMR (151 MHz, D_2O) δ 181.5, 169.9, 165.9, 154.2, 144.2, 131.4, 128.8, 128.3, 126.5, 124.6, 123.1, 117.0, 101.0, 97.7, 75.3, 72.6, 70.5, 70.3, 69.5, 69.0, 68.5, 64.9, 64.7, 63.7, 63.1, 60.7, 52.4, 49.8, 36.6, 28.7, 23.3. ^{31}P NMR (202 MHz, D_2O) δ 0.59, 0.31, -0.75, -1.00 (PO). MALDI-TOF MS (negative mode, THAP): m/z calcd for $C_{147}H_{203}N_{31}O_{74}P_5$ $[M-H]^-$ 3743.25, found 3743.27, MALDI-TOF MS (positive mode, THAP): m/z calcd for $C_{147}H_{205}N_{31}O_{74}P_5$ $[M+H]^+$ 3745.27, found 3745.75. HR-ESI-QToF MS (positive mode): m/z calcd for $C_{147}H_{207}N_{31}O_{74}P_5$ $[(M + 3H)/3]^+$ 1248.4020, found 1248.4016.

Fluorescence quantification of bacterial labelling by cy3-galacto/fucoclusters.

Stationary phase growing bacteria were adjusted to an OD_{620nm} of 3 in PBS 1X and labelled with 10 µg/mL of 4′,6′-diamidino-2-phenylindole (DAPI, Sigma). 1 µM of cy3-galacto/fucoclusters harbouring 0 to 3 catechols/hydroxamates was added to the bacterial suspension and allow to interact for 1h. Initial fluorescence (Cy3 and DAPI) associated with each sample was measured using a Clariostar microplate reader (BMG Labtech). Samples were centrifuged (5000 g, 3 min) and washed in PBS 1X until Cy3 fluorescence of the supernatant was undetectable. Cy3 (ex. 550 nm/em. 570 nm) and DAPI (ex. 350 nm/em. 460 nm) fluorescence of each bacterial suspension was finally measured using the Clariostar fluorescence plate reader. Ratio of Cy3/DAPI fluorescence was considered as specific bacterial labelling by the cy3-galacto/fucoclusters with or w/o catechols or hydroxamate and adjusted to 100% for the control labelling (G0 or F0). Correction of the labelling ratio was done if the initial Cy3 fluorescence of samples were different.

Bacterial and cell culture

The mucoepidermoid pulmonary carcinoma cell line NCI-H292 (A.T.C.C. cell line CRL-1848) was kindly provided by Dr Jean-Marc Lo Guidice (EA4483, Lille, France). Cells were grown in DMEM (Dulbecco's Modified Eagle Medium, Biowest, Denmark) supplemented with 10% (v/v) fetal calf

serum (FCS, Gibco BRL, USA), 2 mM Ultraglutamine (Lonza, Switzerland), 100 units/mL penicillin, and 0.1 mg/mL streptomycin in a humidified atmosphere of 5% CO_2 at 37 °C. For maintenance, cells were grown to confluence and subcultured every 2–3 days at a split ratio of 1:4.
PA strains, wild type PAO1 (kindly provided by Pr. Reuben Ramphal, University of Florida Gainsville, FL, USA) and *lecA*, *lecB*, *fpvA* or *exbB1* mutants (obtained from the Pseudomonas Transposon Mutant Collection, UW Genome Sciences, Washington, USA) were cultured for 16 h at 37 °C in LB medium under 150 rev/min agitation. For adhesion assays, bacteria were washed in DMEM medium without FCS and diluted in the same medium at working concentrations ($1x10^6$ UFC/mL)

Infection assays/Gentamicin protection assay

NCI-H292 cells were seeded into 12-well plates and grown to 80% confluence for 48-72 h in complete DMEM. Medium was renewed every 24h. After two washes with fresh DMEM without FCS, cells were incubated with bacterial suspension in the same medium ($1×10^6$ UFC/mL and MOI of 5) for 2 h at 37 °C. Unbound bacteria were removed by two washes with 1 ml of DMEM without FCS. Then, cells were incubated 1h with fresh DMEM, without FCS, complemented with gentamcin (200 μg/mL) in order to kill bound bacteria not internalized in the cell. Cells were washed four more times with DMEM without FCS, and lysed using deionized water containing 0.02% Triton X-100. Serial dilution of cell lysates in DPBS were then prepared and plated on to LB agar to quantify the rate of infection by comparison with the control, untreated PAO1.
When indicated, galactoclusters with or w/o catechols, were added to the medium during the 2h of infection to a final concentration ranging from 100 to 500 μM.

Statistical analysis

Values presented for fluorescence quantification and Infection assays are means ± SD of three independent experiments and were tested by One-way ANOVA multiple comparison, Tukey-Test, using GraphPad Prism 8.4.

ACKNOWLEDGMENTS

We thank the Agence Nationale de la Recherche "investissements d'avenir" LABEX CheMISyst, ANR-10-LABX-05-01 for financial support and for the award of a research studentship of M.M. F. M. is a member of Inserm.

Conflict of interest

The authors declare no conflict of interest.

[1] C. T. Walsh and T. A. Wencewicz, *Nat. Prod. Rep.* **2013**, *30*, 175-200.

[2] A. Bernardi, J. Jimenez-Barbero, A. Casnati, C. De Castro, T. Darbre, F. Fieschi, J. Finne, H. Funken, K.-E. Jaeger, M. Lahmann, T. K. Lindhorst, M. Marradi, P. Messner, A. Molinaro, P. V. Murphy, C. Nativi, S. Oscarson, S. Penades, F. Peri, R. J. Pieters, O. Renaudet, J.-L. Reymond, B. Richichi, J. Rojo, F. Sansone, C. Schaeffer, W. B. Turnbull, T. Velasco-Torrijos, S. Vidal, S. Vincent, T. Wennekes, H. Zuilhof and A. Imberty, *Chem. Soc. Rev.* **2013**, *42*, 4709-4727.

[3] J. J. Lundquist and E. J. Toone, *Chem. Rev.* **2002**, *102*, 555-578.

[4] a) F. D. Sottile, T. J. Marrie, D. S. Prough, C. D. Hobgood, D. J. Gower, L. X. Webb, J. W. Costerton and A. G. Gristina, *Crit. Care Med.* **1986**, *14*, 265-270; b) J. L. Vincent, D. J. Bihari, P. M. Suter, H. A. Bruining, J. White, R., M. H. Nicolas-Chanoin, M. Wolff, R. C. Spencer and M. Hemmer, *J. Am. Med. Assoc.* **1995**, *274*, 639-644.

[5] a) N. Garber, U. Guempel, A. Belz, N. Gilboagarber and R. J. Doyle, *Biochim. Biophys. Acta* **1992**, *1116*, 331-333; b) E. Mitchell, C. Houles, D. Sudakevitz, M. Wimmerova, C. Gautier, S. Perez, A. M. Wu, N. Gilboa-Garber and A. Imberty, *Nat. Struct. Biol.* **2002**, *9*, 918-921; c) G. Cioci, E. P. Mitchell, C. Gautier, M. Wimmerova, D. Sudakevitz, S. Perez, N. Gilboa-Garber and A. Imberty, *FEBS Lett.* **2003**, *555*, 297-301; d) R. Loris, D. Tielker, K. E. Jaeger and L. Wyns, *J. Mol. Biol.* **2003**, *331*, 861-870; e) A. Imberty, M. Wimmerova, E. P. Mitchell and N. Gilboa-Garber, *Microbes Infect.* **2004**, *6*, 221-228; f) D. Tielker, S. Hacker, R. Loris, M. Strathmann, J. Wingender, S. Wilhelm, F. Rosenau and K. E. Jaeger, *Microbiology* **2005**, *151*, 1313-1323.

[6] a) C. Chemani, A. Imberty, S. de Bentzmann, M. Pierre, M. Wimmerova, B. P. Guery and K. Faure, *Infect. Immun.* **2009**, *77*, 2065-2075; b) T. Eierhoff, B. Bastian, R. Thuenauer, J. Madl, A. Audfray, S. Aigal, S. Juillot, G. E. Rydell, S. Mueller, S. de Bentzmann, A. Imberty, C. Fleck and W. Roemer, *Proc. Natl. Acad. Sci. U. S. A.* **2014**, *111*, 12895-12900.

[7] J. Glick and N. Garber, *J. Gen. Microbiol.* **1983**, *129*, 3085-3090.

[8] a) S. Cecioni, A. Imberty and S. Vidal, *Chem. Rev.* **2015**, *115*, 525-561; b) C. Ligeour, O. Vidal, L. Dupin, F. Casoni, E. Gillon, A. Meyer, S. Vidal, G. Vergoten, J. M. Lacroix, E. Souteyrand, A. Imberty, J. J. Vasseur, Y. Chevolot and F. Morvan, *Org. Biomol. Chem.* **2015**, *13*, 8433-8444; c) R. Visini, X. Jin, M. Bergmann, G. Michaud, F. Pertici, O. Fu, A. Pukin, T. R. Branson, D. M. E. Thies-Weesie, J. Kemmink, E. Gillon, A. Imberty, A. Stocker, T. Darbre, R. J. Pieters and J.-L. Reymond, *ACS Chem. Biol.* **2015**, *10*, 2455-2462; d) G. Michaud, R. Visini, M. Bergmann, G. Salerno, R. Bosco, E. Gillon, B. Richichi, C. Nativi, A. Imberty, A. Stocker, T. Darbre and J.-L.

Reymond, *Chem. Sci.* **2016**, *7*, 166-182; e) A. Angeli, L. Dupin, M. Madaoui, M. Li, G. Vergoten, S. Wang, A. Meyer, T. Gehin, S. Vidal, J.-J. Vasseur, Y. Chevolot and F. Morvan, *Chemistryselect* **2017**, *2*, 10420-10427; f) K. Buffet, I. Nierengarten, N. Galanos, E. Gillon, M. Holler, A. Imberty, S. E. Matthews, S. Vidal, S. P. Vincent and J.-F. Nierengarten, *Chem. Eur. J.* **2016**, *22*, 2955-2963; g) A. Angeli, M. Li, L. Dupin, G. Vergoten, M. Noel, M. Madaoui, S. Wang, A. Meyer, T. Gehin, S. Vidal, J.-J. Vasseur, Y. Chevolot and F. Morvan, *Chembiochem* **2017**, *18*, 1036-1047; h) M. Donnier-Marechal, S. Abdullayev, M. Bauduin, Y. Pascal, M.-Q. Fu, X.-P. He, E. Gillon, A. Imberty, E. Kipnis, R. Dessein and S. Vidal, *Org. Biomol. Chem.* **2018**, *16*, 8804-8809; i) K. S. Buecher, N. Babic, T. Freichel, F. Kovacic and L. Hartmann, *Macromol. Biosci.* **2018**, *18*; j) G. Yu, D. M. E. Thies-Weesie and R. J. Pieters, *Helv. Chim. Acta* **2019**, *102*; k) G. Yu, A. C. Vicini and R. J. Pieters, *J. Org. Chem.* **2019**, *84*, 2470-2488; l) D. Goyard, B. Thomas, E. Gillon, A. Imberty and O. Renaudet, *Front. Chem.* **2019**, *7*.

[9] a) A. M. Boukerb, A. Rousset, N. Galanos, J. B. Mear, M. Thepaut, T. Grandjean, E. Gillon, S. Cecioni, C. Abderrahmen, K. Faure, D. Redelberger, E. Kipnis, R. Dessein, S. Havet, B. Darblade, S. E. Matthews, S. de Bentzmann, B. Guery, B. Cournoyer, A. Imberty and S. Vidal, *J. Med. Chem.* **2014**, *57*, 10275-10289; b) A. Palmioli, P. Sperandeo, A. Polissi and C. Airoldi, *Chembiochem* **2019**, *20*, 2911-2915; c) M. Taouai, K. Chakroun, R. Sommer, G. Michaud, D. Giacalone, M. A. Ben Maaouia, A. Vallin-Butruille, D. Mathiron, R. Abidi, T. Darbre, P. J. Cragg, C. Mullie, J.-L. Reymond, G. A. O'Toole and M. Benazza, *J. Med. Chem.* **2019**, *62*, 7722-7738; d) G. Granata, S. Stracquadanio, G. M. L. Consoli, V. Cafiso, S. Stefani and C. Geraci, *Carbohydr. Res.* **2019**, *476*, 60-64.

[10] a) M. Donnier-Marechal, N. Galanos, T. Grandjean, Y. Pascal, D.-K. Ji, L. Dong, E. Gillon, X.-P. He, A. Imberty, E. Kipnis, R. Dessein and S. Vidal, *Org. Biomol. Chem.* **2017**, *15*, 10037-10043; b) F. Zuttion, C. Ligeour, O. Vidal, M. Waelte, F. Morvan, S. Vidal, J.-J. Vasseur, Y. Chevolot, M. Phaner-Goutorbe and H. Schillers, *Nanoscale* **2018**, *10*, 12771-12778; c) L. Malinovska, L. Son Thai, M. Herczeg, M. Vaakova, J. Houser, E. Fujdiarova, J. Komarek, P. Hodek, A. Borbas, M. Wimmerova and M. Csavas, *Biomolecules* **2019**, *9*.

[11] a) B. Gerland, A. Goudot, G. Pourceau, A. Meyer, V. Dugas, S. Cecioni, S. Vidal, E. Souteyrand, J. J. Vasseur, Y. Chevolot and F. Morvan, *Bioconjugate Chem.* **2012**, *23*, 1534-1547; b) B. Gerland, A. Goudot, C. Ligeour, G. Pourceau, A. Meyer, S. Vidal, T. Gehin, O. Vidal, E. Souteyrand, J. J. Vasseur, Y. Chevolot and F. Morvan, *Bioconjugate Chem.* **2014**, *25*, 379-392.

[12] a) M. Miethke and M. A. Marahiel, *Microbiol. Mol. Biol. Rev.* **2007**, *71*, 413-451; b) H. Drakesmith and A. Prentice, *Nat. Rev. Microbiol.* **2008**, *6*, 541-552.

[13] R. C. Hider and X. L. Kong, *Nat. Prod. Rep.* **2010**, *27*, 637-657.

[14] I. J. Schalk and L. Guillon, *Amino Acids* **2013**, *44*, 1267-1277.

[15] a) C. Ji, R. E. Juarez-Hernandez and M. J. Miller, *Future Med. Chem.* **2012**, *4*, 297-313; b) S. Rebuffat, *Biochem. Soc. Trans.* **2012**, *40*, 1456-1462; c) G. L. A. Mislin and I. J. Schalk, *Metallomics* **2014**, *6*, 408-420; d) T. F. Zheng, J. L. Bullock and E. M. Nolan, *J. Am. Chem. Soc.* **2012**, *134*, 18388-18400; e) T. F. Zheng and E. M. Nolan, *J. Am. Chem. Soc.* **2014**, *136*, 9677-9691; f) P. Chairatana, T. F. Zheng and E. M. Nolan, *Chem. Sci.* **2015**, *6*, 4458-4471.

[16] P. Cornelis and J. Dingemans, *Front.Cell.Infect.Microbiol.* **2013**, *3*.

[17] G. Pourceau, A. Meyer, Y. Chevolot, E. Souteyrand, J. J. Vasseur and F. Morvan, *Bioconjugate Chem.* **2010**, *21*, 1520-1529.

[18] Z. H. Zhang, Y. Yu and L. S. Liebeskind, *Org. Lett.* **2008**, *10*, 3005-3008.

[19] J. Lietard, A. Meyer, J. J. Vasseur and F. Morvan, *J. Org. Chem.* **2008**, *73*, 191-200.

[20] T. Hasegawa, M. Numata, S. Okumura, T. Kimura, K. Sakurai and S. Shinkai, *Org. Biomol. Chem.* **2007**, *5* 2404-2412.

[21] G. Pourceau, A. Meyer, J. J. Vasseur and F. Morvan, *J. Org. Chem.* **2009**, *74*, 6837-6842.

[22] J. Katajisto, P. Virta and H. Lonnberg, *Bioconjugate Chem.* **2004**, *15*, 890-896.

[23] C. Ligeour, A. Meyer, J. J. Vasseur and F. Morvan, *Eur. J. Org. Chem.* **2012**, 1851-1856.

[24] F. Morvan, A. Meyer, A. Jochum, C. Sabin, Y. Chevolot, A. Imberty, J. P. Praly, J. J. Vasseur, E. Souteyrand and S. Vidal, *Bioconjugate Chem.* **2007**, *18*, 1637-1643.

[25] H.-P. Wu, T.-L. Cheng and W.-L. Tseng, *Langmuir* **2007**, *23*, 7880-7885.

[26] J. Greenwald, M. Nader, H. Celia, C. Gruffaz, V. Geoffroy, J. M. Meyer, I. J. Schalk and F. Pattus, *Mol. Microbiol.* **2009**, *72*, 1246-1259.

[27] a) A. Ito, T. Nishikawa, S. Matsumoto, H. Yoshizawa, T. Sato, R. Nakamura, M. Tsuji and Y. Yamano, *Antimicrob. Agents Chemother.* **2016**, *60*, 7396-7401; b) G. G. Zhanel, A. R. Golden, S. Zelenitsky, K. Wiebe, C. K. Lawrence, H. J. Adam, T. Idowu, R. Domalaon, F. Schweizer, M. A. Zhanel, P. R. S. Lagace-Wiens, A. J. Walkty, A. Noreddin, J. P. Lynch and J. A. Karlowsky, *Drugs* **2019**, *79*, 271-289.

[28] E. K. Dolence, C. E. Lin, M. J. Miller and S. M. Payne, *J. Med. Chem.* **1991**, *34*, 956-968.

[29] N. Noinaj, M. Guillier, T. J. Barnard and S. K. Buchanan in *TonB-Dependent Transporters: Regulation, Structure, and Function, Vol. 64* Eds.: S. Gottesman and C. S. Harwood), **2010**, pp. 43-60.

[30] S. P. Diggle, R. E. Stacey, C. Dodd, M. Camara, P. Williams and K. Winzer, *Environ. Microbiol.* **2006**, *8*, 1095-1104.

[31] V. Percec, P. Leowanawat, H. J. Sun, O. Kulikov, C. D. Nusbaum, T. M. Tran, A. Bertin, D. A. Wilson, M. Peterca, S. D. Zhang, N. P. Kamat, K. Vargo, D. Moock, E. D. Johnston, D. A. Hammer, D. J. Pochan, Y. C. Chen, Y. M. Chabre, T. C. Shiao, M. Bergeron-Brlek, S. Andre, R. Roy, H. J. Gabius and P. A. Heiney, *J. Am. Chem. Soc.* **2013**, *135*, 9055-9077.

[32] O. Bajolet-Laudinat, S. Girod-de Bentzmann, J. M. Tournier, C. Madoulet, M. C. Plotkowski, C. Chippaux and E. Puchelle, *Infect. Immun.* **1994**, *62*, 4481-4487.
[33] W. H. A. Kuijpers and C. A. A. Vanboeckel, *Tetrahedron* **1993**, *49*, 10931-10944.